Supplemental Materials

Molecular Biology of the Cell

Jalihal *et al*.

S1 Model Construction

The Standard Component Modeling (SCM) framework used to create our model of nutrient signaling is described here in brief. SCM classifies biochemical reactions based on their time scales. The slow timescale reactions (*Class I*) are represented by mass-action rate laws

$$\frac{d[\mathrm{A}]}{dt} = k_p - k_d[\mathrm{A}], \tag{1}$$

where k_p is the rate of production and k_d is the rate of degradation of species A.

The intermediate timescale reactions (*Class II*) are represented by a generic, sigmoidal, 'soft-Heaviside' function. For example, a protein P undergoing a post-translational modification would be described by the differential equation

$$\frac{d[\mathrm{P}]}{dt} = \gamma([\mathrm{P_T}]\mathcal{H}(\sigma, w) - [\mathrm{P}]), \tag{2}$$

where $[\mathrm{P_T}]$ represents the total amount of species P, and $\mathcal{H}$ is the soft-Heaviside function, given by

$$\mathcal{H}(\sigma, W) = \frac{1}{1 + e^{-\sigma W}}, \qquad W = \omega_0 + \sum_{i=1}^{N} \omega_i[\mathrm{X}_i]$$

$\mathcal{H}$ is a sigmoid function used to represent a switch-like biochemical mechanism. Here the W term is composed of a linear combination of the concentrations of the regulators X_i of P with appropriate signed coefficients ω_i, along with a scaling factor σ which determines the steepness of the response. The γ parameter governs the time scale of this reaction. In this work, $[\mathrm{P_T}] = 1$ for every *Class II* variable in a wild-type cell, and we set $[\mathrm{P_T}] = 0$ to simulate a cell deleted for the gene encoding P. Thus, the value of a *Class II* variable, which lies between 0 and 1, denotes the fraction of the given signaling component in a particular post-translational modification state.

Finally the reactions occurring on fast time scales, such as the formation of protein complexes, are represented by the *Class III* equations governed by the stoichiometric relationships between the constituents of the protein complexes. Thus, the stoichiometric association of components X and Y to produce a complex C would be represented as

$$C = \min(X, Y) \tag{3}$$

The kinetic expressions defining the ODE model are presented in the next section. A majority of the expressions (21 out of 25) are *Class II* equations. The model has four *Class I* equations, describing the dynamics of Glutamine and cAMP, Ribosomal components (Rib), and Protein accumulation. Finally the model has two *Class III* equations: First, the charging of tRNAs as a fast association between total uncharged tRNAs and intracellular amino acids, represented by Glutamine. Second, the assembly of active Ribosomes (aRib) is represented as the fast association of Ribosomal components (Rib) and unphosphorylated initiation factor eIF2α.

S1.1 Kinetic expressions

Nutrient signal sensing and transduction

$$\frac{d[\text{Glutamine}]}{dt} = (k_{acc-glu}[\text{Glutamine}_{ext}] + k_{acc-pro}\text{Proline} + k_{acc-nh4}\text{NH}_4[\text{Gln1}]\text{Carbon}) - k_{degr}[\text{Glutamine}]$$

$$\frac{d[\text{Cyr1}]}{dt} = \gamma_{cyr}([\text{Cyr1}_\text{T}]\mathcal{H}(\sigma_{cyr}, \omega_{cyr-glu}\text{Carbon}[\text{Ras}] - \omega_{cyr} - \omega_{cyr-snf}[\text{Snf1}]) - [\text{Cyr1}])$$

$$\frac{d[\text{Ras}]}{dt} = \gamma_{ras}([\text{Ras}_\text{T}]\mathcal{H}(\sigma_{ras}, -\omega_{ras-pka}[\text{PKA}] + \omega_{ras-glu}\text{Carbon} + \omega_{ras)} - [\text{Ras}])$$

$$\frac{d[\text{EGO}]}{dt} = \gamma_{ego}([\text{EGO}_\text{T}]\mathcal{H}(\sigma_{ego}, \omega_{ego-gap}[\text{EGOGAP}]([\text{Glutamine}]_{ext} + 0.5\text{NH}_4 + 0.01\text{Proline}) - \omega_{ego}(1 - [\text{Glutamine}]) - \omega_{ego-basal}) - [\text{EGO}])$$

$$\frac{d[\text{EGOGAP}]}{dt} = \gamma_{gap}([\text{EGOGAP}_\text{T}]\mathcal{H}(\sigma_{gap}, \omega_{gap-N}(1 - [\text{Glutamine}]) - \omega_{gap-torc}[\text{TORC1}]) - [\text{EGOGAP}])$$

$$\frac{d[\text{cAMP}]}{dt} = k_{camp-cyr}[\text{Cyr1}]ATP - k_{camp-pde}[\text{PDE}][\text{cAMP}] - k_{camp-deg}[\text{cAMP}]$$

$$\frac{d[\text{PDE}]}{dt} = \gamma_{pde}([\text{PDE}_\text{T}]\mathcal{H}(\sigma_{pde}, \omega_{pde-pka}[\text{PKA}] - \omega_{pde)} - [\text{PDE}])$$

$$\frac{d[\text{Sak}]}{dt} = [\text{Sak}_\text{T}]\mathcal{H}(\sigma_{sak}, \omega_{sak} - \omega_{sak-pka}[\text{PKA}]) - [\text{Sak}]$$

Master regulators

$$\frac{d[\text{TORC1}]}{dt} = \gamma_{tor}([\text{TORC1}_\text{T}]\mathcal{H}(\sigma_{tor}, \omega_{torc-glut}[\text{Glutamine}] + \omega_{torc-ego}[\text{EGO}] - \omega_{torc-egoin}(1 - [\text{EGO}]) - \omega_{torc} - \omega_{torc-snf}[\text{Snf1}]) - [\text{TORC1}])$$

$$\frac{d[\text{Snf1}]}{dt} = \gamma_{snf}([\text{Snf1}_\text{T}]\mathcal{H}(\sigma_{snf}, -\omega_{snf-glc}\text{Carbon} + \omega_{snf-sak}[\text{Sak}] - \omega_{snf)} - [\text{Snf1}])$$

$$\frac{d[\text{PKA}]}{dt} = \gamma_{pka}([\text{PKA}_\text{T}]\mathcal{H}(\sigma_{pka}, \omega_{pka-camp}[\text{cAMP}] - \omega_{pka} - \omega_{pka-sch9}[\text{Sch9}]) - [\text{PKA}])$$

$$\frac{d[\text{Sch9}]}{dt} = \gamma_{sch9}([\text{Sch9}_\text{T}]\mathcal{H}(\sigma_{sch9}, \omega_{sch9-torc}[\text{TORC1}] - \omega_{sch9)} - [\text{Sch9}])$$

Downstream responses

$$
\begin{aligned}
\frac{d[\text{Gcn2}]}{dt} &= \gamma_{gcn2}([\text{Gcn2}_\text{T}]\mathcal{H}(\sigma_{gcn2}, \omega_{gcn} - \omega_{gcn-torc}[\text{Sch9}]) - [\text{Gcn2}]) \\
\frac{d[\text{Gcn4}]}{dt} &= \gamma_{gcn4}([\text{Gcn4}_\text{T}]\mathcal{H}(\sigma_{gcn4}, \\
&\qquad \omega_{gcn4-gcn2-trna}\min([\text{Gcn2}], 74.5([\text{tRNA}_\text{total}] - \min([\text{tRNA}_\text{total}], [\text{Glutamine}]))) \\
&\qquad - \omega_{gcn4)} - [\text{Gcn4}]) \\
\frac{d[\text{eIF}]}{dt} &= \gamma_{eif}([\text{eIF}_\text{T}]\mathcal{H}(\sigma_{eif}, \omega_{eif} - \omega_{eif-gcn2}[\text{Gcn2}]) - [\text{eIF}]) \\
\frac{d[\text{Gln3}]}{dt} &= \gamma_{gln3}([\text{Gln3}_\text{T}]\mathcal{H}(\sigma_{gln}, -\omega_{gln3} + \omega_{gln-snf}[\text{Snf1}] + \omega_{gln-sit}(1 - [\text{TORC1}])) - [\text{Gln3}]) \\
\frac{d[\text{Gln1}]}{dt} &= \gamma_{gln1}([\text{Gln1}_\text{T}]\mathcal{H}(\sigma_{gln1}, \omega_{gln1-gln3}[\text{Gln3}] - \omega_{gln1)} - [\text{Gln1}]) \\
\frac{d[\text{Rtg13}]}{dt} &= \gamma_{rtg13}([\text{Rtg13}_\text{T}]\mathcal{H}(\sigma_{rtg}, -\omega_{rtg-torc}[\text{TORC1}] + \omega_{rtg)} - [\text{Rtg13}]) \\
\frac{d[\text{Gis1}]}{dt} &= \gamma_{gis1}([\text{Gis1}_\text{T}]\mathcal{H}(\sigma_{gis1}, -\omega_{gis-pka}[\text{PKA}] - \omega_{gis-sch}[\text{Sch9}] + \omega_{gis)} - [\text{Gis1}]) \\
\frac{d[\text{Mig1}]}{dt} &= \gamma_{mig}([\text{Mig1}_\text{T}]\mathcal{H}(\sigma_{mig1}, \omega_{mig-pka}[\text{PKA}] - \omega_{mig-snf}[\text{Snf1}] + \omega_{mig)} - [\text{Mig1}]) \\
\frac{d[\text{Dot6}]}{dt} &= \gamma_{dot6}([\text{Dot6}_\text{T}]\mathcal{H}(\sigma_{dot}, -\omega_{dot-sch-pka}[\text{Sch9}][\text{PKA}] + \omega_{dot)} - [\text{Dot6}]) \\
\frac{d[\text{Tps1}]}{dt} &= \gamma_{tps}([\text{Tps1}_\text{T}]\mathcal{H}(\sigma_{tps}, \omega_{tps-pka}([\text{PKA}_\text{T}] - [\text{PKA}]) - \omega_{tps)} - [\text{Tps1}]) \\
\frac{d[\text{Trehalase}]}{dt} &= \gamma_{tre}([\text{Trehalase}_\text{T}]\mathcal{H}(\sigma_{trehalase}, \omega_{tre-pka}[\text{PKA}] - \omega_{tre)} - [\text{Trehalase}]) \\
\frac{d[\text{Protein}]}{dt} &= k_{pr}[\text{ATP}]\min(\min([\text{Rib}], [\text{eIF}]), \min([\text{tRNA}_\text{total}], [\text{Glutamine}]))[\text{Protein}] \\
\frac{d[\text{Rib}]}{dt} &= k_{\text{transcription}}(1 - [\text{Dot6}]) - k_{mRNA-degr}[\text{Rib}]
\end{aligned}
$$

Some heuristics have been used in order to model the following components.

Amino acid sensing The detailed mechanism of amino acid sensing is beyond the scope of this model. In order to simplify this pathway, it is assumed that the EGO complex integrates all nitrogen signals. Thus the activation of the EGO complex is determined by the strength of the activating signal, which is represented by

$$[\text{Glutamine}_{ext}] + 0.5[\text{NH}_4] + 0.01[\text{Proline}]$$

with the coefficients being derived from best fits to Sch9 activation data from [30].

Ribosome Biogenesis Here we abstract away the complexities of the synthesis of ribosome components and represent the 'synthesis' of ribosomes by a mass action law, regulated by the RIBI repressor Dot6.

$$\frac{d[\text{Rib}]}{dt} = k_{\text{transcription}}(1 - [\text{Dot6}]) - k_{\text{mRNA\_degr}}[\text{Rib}]$$

Protein Translation We abstract away the complexities of ribosome assembly and assume that a ribosome is functional when a stoichiometric ratio of the ribosomal precursor (Rib), charged tRNA, and unphosphorylated initiation factor eIF2α is present.

$$\frac{d[\text{Protein}]}{dt} = k_{pr}[\text{ATP}]\min(\text{aRib}, \text{tRNA}^*)[\text{Protein}]$$

$$\mathrm{tRNA}^* = \min(\mathrm{tRNA}_{\mathrm{total}}, \mathrm{Glutamine})$$

$$\mathrm{aRib} = \min(\mathrm{Rib}, \mathrm{eIF}),$$

where tRNA^* represents the charged tRNA pool, and aRib represents the actively translating ribosomes.

The experimental data used to calibrate the model comprises genetic perturbations to individual catalytic subunits of the complex regulators. For the most part, it is beyond the scope of the current model to represent the activities of individual subunits, and we treat a regulatory complex as a single entity in the model. However, this assumption fails in cases where experimental evidence indicates that the catalytic subunits have distinct activities. We discuss two such instances below.

- PKA has three catalytic subunits Tpk1, Tpk2, and Tpk3. Experimental data from strains with single Tpk subunits (cf. Mbonyi *et al.* 1990) indicate that each of these subunits have distinct catalytic activities, where TPK1 and TPK3 exhibit similar activities, while TPK2 is similar to *wt*. The model currently is able to capture the phenotypes of strains with Tpk1 and Tpk3 subunits by setting the total amount of PKA to 0.3 of the *wt* activity. However this assumption is not sufficient to model the strain with a single Tpk2 subunit, and we currently do not attempt to model the Tpk2 subunit of PKA.
- PDE has two catalytic subunits, Pde1 and Pde2. The *pde1*Δ, *pde2*Δ, and the *pde1*Δ*pde2*Δ strains all show very different cAMP phenotypes with respect to glucose upshifts (cf. Ma 1999, Figure 1A). Our model succeeds in capturing the phenotype of only the *pde1*Δ strain, i.e. the PDE2 subunit. We do not attempt to model the *pde2*Δ strain.

In both the above cases, a single model representation is unable to explain the behavior of various catalytic subunits. A goal for a future version of the model is to incorporate data specific to various subunits by uniquely representing the various genetic mutant strains.

S2 Robustness analysis

This section describes the details of the parameter robustness analysis. The motivation for this analysis is the concept of model sloppiness developed by Gutenkunst *et al.*, 2007 [78] who investigated the characteristics of a cost function quantifying the deviation of model predictions from a set of experimental data. The value of the cost function depends on the values of the parameters in the model. In their investigations Gutekunst *et al.* found that the cost as a function of model parameters typically exhibits a 'stiff/sloppy' structure, i.e., while one can identify a few parameter combinations that tightly constrain the cost function, a majority of parameter combinations do not significantly constrain the cost function. Here, we are interested in the so-called stiff parameter directions, which are highly constrained by data. We carry out this investigation in the following stages:

1. We define a cost function that measures the fit between the experimental data and model predictions, described in Section S2.1.
2. We use the cost function to improve the global fit of the model to the data using an MCMC sampling strategy described in Section S2.2.
3. We approximate the structure of this cost function in parameter space by computing the Hessian of this surface around the optimal parameter set using the method described in [79]. Details of this method are provided in Section S2.3.
4. We generate a sample of parameter sets constrained by the eigenvectors of the Hessian matrix, and iteratively refine the Hessian, as described in Sections S2.4,S2.5.
5. Finally, we study the properties of this refined Hessian to identify the stiff and sloppy parameter directions in our model, given the set of curated experimental data used to constrain the model. This is described in Sections S2.7S2.6S2.8S2.9.

S2.1 The goodness-of-fit cost function

This quadratic cost function $C(\mathbf{p})$, which includes both the time series data and the steady-state pertubation data as described in 'Results', is defined as follows:

$$C(\mathbf{p}) = \frac{1}{N}\sum_{i}^{N}(y_i^t(\mathbf{p}) - x_i^t)^2 + \frac{1}{M}\sum_{i}^{M}(y_i^u(\mathbf{p}) - x_i^u)^2, \tag{4}$$

where N is the number of time points (t) and M the number of perturbations (u), $\mathbf{p}$ is the candidate parameter vector, $y(\mathbf{p})$ is the model prediction and x is the literature-derived activity of the variable under consideration. While the number of time points exceed the number of perturbation data points, we do not preferentially weight one type of data over the other.

S2.2 MCMC sampling to improve estimate of parameter values

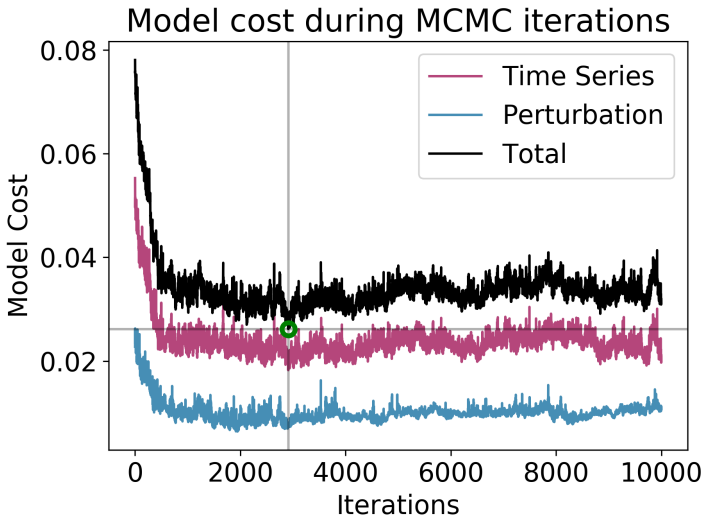

Figure S1: Results of MCMC sampling. The black line shows the total model cost. The contributions from the time course term and from the perturbation term are shown in pink and blue, respectively. The lowest cost, designated by the green circle at iteration 2900, defines the 'optimal' parameter set.

Having defined the quadratic cost function, we used a Markov Chain Monte Carlo (MCMC) sampling strategy to improve the fit to the data. Briefly, in every MCMC iteration, the last accepted parameter set is perturbed as follows: for each parameter with value p in the last accepted set, a new value p' is sampled from a normal distribution $\mathcal{N}(\mu = p, \sigma = 0.025p)$. The cost function is evaluated for this new parameter set and this set is accepted with probability $e^{-\beta\Delta C}$, where $\Delta C = C(p') - C(p)$. We chose $\beta = 3.6$ based on the magnitude of the change in cost that we observed in each iteration. Starting from the hand-tuned parameter set, we repeat MCMC sampling 10,000 times. The change in cost across the iterations is shown in Figure S1.

S2.3 Defining a Hessian approximation based on a sample of parameter sets

In this section, we derive the expressions used to compute the Hessian.

Let $\mathbf{p}^*$ denote the parameter set that minimizes $C(\mathbf{p})$, i.e., $C(\mathbf{p}^*) = C_{\min}$, then

$$\nabla C(\mathbf{p})|_{\mathbf{p}^*} = 0.$$

Thus, for every $\mathbf{p}$ in the neighborhood of $\mathbf{p}^*$, we can carry out a Taylor series expansion around $\mathbf{p}^*$. Omitting the higher order terms:

$$C(\mathbf{p}) \approx C(\mathbf{p}^*) + (\mathbf{p} - \mathbf{p}^*)^T H(\mathbf{p} - \mathbf{p}^*) = C(\mathbf{p}^*) + \Delta\mathbf{p}^T H \Delta\mathbf{p}, \tag{5}$$

where $2H = \nabla^2 C$ is the Hessian of the cost function.

Next, we define some notation as introduced in Magnus and Neudecker [94]. For an $m \times n$ matrix A, the vectorization operation $\text{vec}(A)$ results in a $mn \times 1$ column vector that stacks the columns of A. If A is an $n \times n$ symmetric matrix, then the operation $\text{vech}(A)$ stacks the lower triangular columns, yielding an $\frac{n(n+1)}{2} \times 1$ column vector. There exists a unique matrix D, called the duplicator matrix, with dimensions $n \times \frac{n(n+1)}{2}$, and a unique matrix L called the eliminator matrix with dimensions $\frac{n(n+1)}{2} \times n^2$, such that

$$\begin{aligned} \text{vec}(A) &= D\,\text{vech}(A) \\ \text{vech}(A) &= L\,\text{vec}(A) \end{aligned}$$

The Kronecker product (denoted by $\otimes$) of an $m \times n$ matrix A and an $s \times t$ matrix B is an $mn \times st$ matrix

$$A \otimes B = (a_{ij})B,$$

where a_{ij} is the ij^{th} entry of A. For any three matrices A, B and C the following holds true

$$\text{vec}(ABC) = (C^T \otimes A)\text{vec}(B)$$

Suppose we choose S parameter sets $\mathbf{p}_i, 1 \leq i \leq S$ in the neighborhood of $\mathbf{p}^*$. We can construct a quadratic error function E_H which will be minimized when H approximates the true Hessian of the function.

$$E_H = \frac{1}{2}\sum_{i=1}^{S}\left(C(\mathbf{p}_i) - C(\mathbf{p}^*) - (\mathbf{p}_i - \mathbf{p}^*)^T H(\mathbf{p}_i - \mathbf{p}^*)\right)^2$$

Using $\Delta C_i = C(\mathbf{p}_i) - C(\mathbf{p}^*)$ and $\Delta\mathbf{p}_i = (\mathbf{p}_i - \mathbf{p}^*)$, we have

$$\frac{\partial E_H}{\partial H} = 0 = \sum_i^S (\Delta C_i - \Delta\mathbf{p}_i^T H \Delta\mathbf{p}_i)\Delta\mathbf{p}_i\Delta\mathbf{p}_i^T \tag{6}$$

We wish to solve for H given a set of parameter vectors $\mathbf{p}$. For a model with k parameters, we will have to solve for k^2 terms in H. However, we can decrease the size of this problem by considering the fact that the Hessian should be a symmetric matrix. Thus, we need to solve only for the terms in the lower triangle.

Simplifying Equation 6, we have

$$\sum_i^S \Delta C_i \Delta \mathbf{p}_i \Delta \mathbf{p}_i^T = \sum_i^S \Delta \mathbf{p}_i^T H \Delta \mathbf{p}_i \Delta \mathbf{p}_i^T$$

$$\begin{aligned}
\sum_i^S \Delta C_i \text{vech}(\Delta \mathbf{p}_i \Delta \mathbf{p}_i^T) &= \sum_i^S (\Delta \mathbf{p}_i^T H \Delta \mathbf{p}_i) \text{vech}(\Delta \mathbf{p}_i \Delta \mathbf{p}_i^T) \\
&= \sum_i^S (\Delta \mathbf{p}_i^T \otimes \Delta \mathbf{p}_i) \text{vec}(H) \text{vech}(\Delta \mathbf{p}_i \Delta \mathbf{p}_i^T) \\
&= \sum_i^S \text{vec}(\Delta \mathbf{p}_i \Delta \mathbf{p}_i^T)^T \text{vec}(H) \text{vech}(\Delta \mathbf{p}_i \Delta \mathbf{p}_i^T) \\
&= \sum_i^S \text{vech}(\Delta \mathbf{p}_i \Delta \mathbf{p}_i^T) D^T D \text{vech(H)} \text{vech}(\Delta \mathbf{p}_i \Delta \mathbf{p}_i^T) \\
&= \sum_i^S \text{vech}(\Delta \mathbf{p}_i \Delta \mathbf{p}_i^T) \text{vech}(\Delta \mathbf{p}_i \Delta \mathbf{p}_i^T)^T D^T D \text{vech}(H) \\
&= \sum_i^S Q D^T D \text{vech}(H) \quad \text{where } Q = \text{vech}(\Delta \mathbf{p}_i \Delta \mathbf{p}_i^T) \text{vech}(\Delta \mathbf{p}_i \Delta \mathbf{p}_i^T)^T
\end{aligned}$$

If we define $R = \sum_i \Delta C_i \text{vech}(\Delta \mathbf{p}_i \Delta \mathbf{p}_i^T)$, we have that

$$R = Q D^T D \text{vech}(H)$$
$$\text{In other words,} \text{vech}(H) = (Q D^T D)^{-1} R$$

and

$$\text{vec}(H) = D(Q D^T D)^{-1} R \tag{7}$$

Here, R is symmetric and D is the appropriate duplicator matrix.

S2.4 Sampling new parameter sets constrained by the approximate Hessian

Using the approximate Hessian matrix computed as described in Equation 7, we next wish to use the eigenvectors of this matrix to contrain the search for new parameter vectors. Intuitively we wish to avoid the eigenvector directions corresponding to 'large' eigenvalues which are the stiff directions. We know that the dimensions of the cost ellipsoids are proportional to $\frac{1}{\lambda^{1/2}}$ where λ is an eigenvalue of the Hessian. Thus we can weight the eigenvectors by a factor of $\frac{1}{\lambda^{1/2}}$, which favors the sloppiest eigenvector directions. In practice we want a candidate parameter vector to respect all the stiff and sloppy directions. We first generate a random vector α, which we then transform to respect the stiff and sloppy directions. We describe the transformation matrix below.

We start by translating the frame of reference our system to $\mathbf{p}^*$ so that we can generate vectors $\Delta \mathbf{p} = \mathbf{p} - \mathbf{p}^*$ which produce a relative increase in model cost $\Delta C = C - C_{\min}$. Rewriting Equation 5,

$$\Delta C(\mathbf{p}) \approx \Delta \mathbf{p}^T H \Delta \mathbf{p}$$

To avoid an ill-conditioned Hessian, where the eigenvalues span many orders of magnitude, we choose $\Delta l_p^T H \Delta l_p = \Delta C$ where $\Delta l_p = \log(\mathbf{p}) - \log(\mathbf{p}^*)$, with the logarithm of a vector being taken elementwise.

To sample from this new ellipsoid, we first create a random vector α which will lie inside the cost ellipsoid. we sample a vector $\tilde{\alpha}$ of random numbers drawn from $\mathcal{N}(0, 1)$. Next, we compute α

$$\alpha = \frac{\tilde{\alpha}}{\sqrt{\tilde{\alpha}^T \tilde{\alpha}}} u \sqrt{\epsilon},$$

where u is a scalar drawn from the uniform distribution on [0,1] and $\epsilon = 2C_{min} = 2 \times 0.026$ is the maximum value of ΔC we wish to consider. The factor $\sqrt{\epsilon}$ scales the magnitude of the unit vector $\frac{\tilde{\alpha}}{\sqrt{\tilde{\alpha}^T \tilde{\alpha}}}$ to the edge of the ellipsoid. The final factor u ensures that the vector lies inside the ellipsoid, as we want to sample the volume, not just the surface of the ellipsoid.

The final step needed to generate a candidate parameter vector is to transform it to respect the stiff and sloppy directions. Using an eigenvalue decomposition, we write $H = V \Lambda V^T$ (where V is the eigenvalue matrix and Λ is the eigenvector matrix). (Note that we compute the absolute values of the eigenvalues and replace every eigenvalue that is less than 0.1 by 0.1. This step ensures that H is positive definite, but limits the length of the longest ellipsoid axes.) Our constrained parameter vector should take the form $\Delta l_p = V \Lambda^{-1/2} \alpha$. This will satisfy the cost constraint as follows

$$\Delta l_p^T H \Delta l_p = \alpha^T \Lambda^{-1/2} V^T V \Lambda V^T V \Lambda^{-1/2} \alpha = \alpha^T \alpha \leq \epsilon$$

Reordering terms, we have

$$\mathbf{p} = e^{\log \mathbf{p}^* + V \Lambda^{1/2} \alpha} = \mathbf{p}^* .* e^{V \Lambda^{-1/2} \alpha} \tag{8}$$

where the $.*$ operator denotes element-wise multiplication, and the exponentiation in the $e^{V \Lambda^{-1/2} \alpha}$ is carried out element-wise.

S2.5 Iterative refinement of the approximate Hessian

The following steps describe our methodology to initialize a approximation to the Hessian and then refine this approximation iteratively.

1. To compute an initial approximation of the Hessian, we used Latin Hypercube Sampling around 2.5%ranges around $\mathbf{p}^*$ in order to sample parameter vectors close to $\mathbf{p}^*$. We evaluated the cost for each parameter set. For each range explored, we recorded the parameter sets with cost less than $2C_{\text{min}}$.

2. Next, using Equation 7, an approximate Hessian was constructed using the accepted parameter sets from the Latin Hypercube sample. This step was designated as iteration 0.

3. Using the approximate Hessian generated in the previous step, 30,000 parameter sets were generated using Equation 8. The goodness-of-fit cost was evaluated for each parameter set and any parameter set satisfying a cost cutoff of $3C_{\text{min}}$ was accepted.

4. Using these accepted parameter sets, the approximate Hessian was recomputed, a new ensemble of 30,000 parameter sets was generated, and the cost evaluation and parameter set acceptance procedure was repeated, while continually expanding the ensemble of accepted parameter sets.

5. The previous step was repeated four times.

In our parameter search we fix the values of the total amounts of protein, the P_T parameters to 1.0 since we currently do not have accurate abundances of the regulators in the model, accounting for 21 parameters. We also set the *sigma* parameters in each *Class II* equation to their nominal values presented in Table S2, accounting for another 21 parameters. Lastly, 5 parameters serve as model inputs, namely ATP, Carbon, Glutamine$_{textext}$, Ammonia, and Proline. Thus we fix the values of 49 of the 128 kinetic parameters, The remaining 81 parameters were varied in this analysis. At the end of the four iterations, we obtained a total of 24,066 parameter sets.

S2.6 Fewer than 16% of the eigenvectors are required to capture all the stiff directions

We studied the eigenvector of the refined-approximate Hessian H in order to identify the parameters that contribute to the stiff directions. We deemed a parameter as making a substantial contribution to an eigenvector if the absolute value of its 'loading' (i.e., its weight in the eigenvector) was greater than one

standard deviation of all the loadings across all eigenvectors. Figure S2(a) shows the number of unique parameters with substantial contributions to the ordered eigenvectors of H. Since we vary 81 parameters, the matrix H has 81 eigenvectors. We observe that 90% (72 of 81) of the parameters make substantial contributions to the first 13 eigenvectors. Thus, all parameters contribute substantially in the first 16% (13 of 81) of the stiff directions.

Finally, we observe an initial slump in the number of unique parameters, implying that only 28 parameters contribute substantially to the first seven stiff directions, i.e., around 34% of the parameters contribute to the stiffest directions, indicated by the red lines in Figure S2(a).

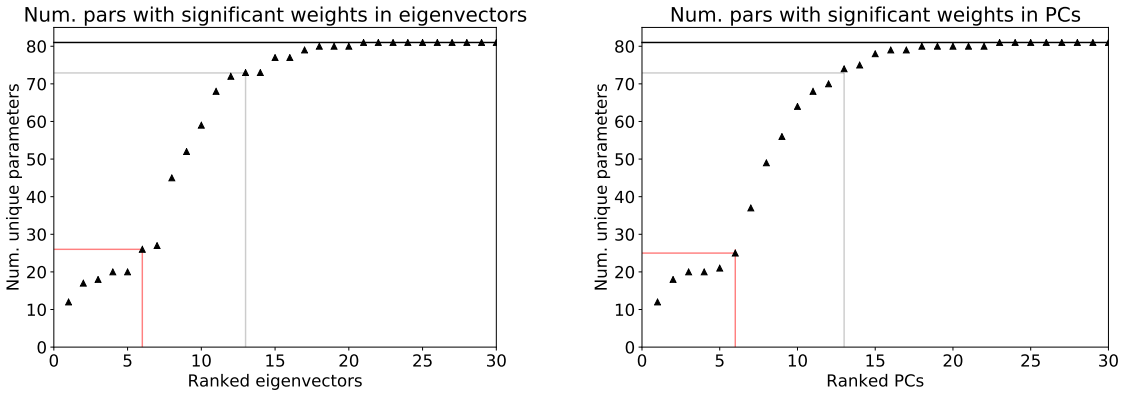

(a) Eigenvectors of H sorted in decreasing order of their corresponding eigenvalue

(b) PCs sorted in increasing order of their explained variance ratio

Figure S2: Comparison between the parameters with high weights in eigenvectors. On the x-axis are the sorted eigenvectors, such that the eigenvector corresponding to the largest eigenvalue gets a rank of 1. Each plot shows the number of unique parameters with substantial coefficients in the each eigenvector. The gray lines mark the number of eigenvectors required to capture 90% of the parameters. The black horizontal line marks the total number of parameters varied in our analysis, namely 81. The plot on the left is derived from the eigenvectors from the approximate Hessian, whereas the plot on the right represents the results from the principal components resulting from carrying out PCA on the collection of parameter sets, i.e., the eigenvectors of the covariance matrix sorted by the inverse of their eigenvalues. The red lines indicate a characteristic inflection point in the trend of parameters contributing substantially to eigenvectors which we interpret as the stiff directions.

S2.7 Comparison between the eigenvectors of the Hessian and the inverse covariance matrix

We also compared the quality of the approximate Hessian derived from our iterative scheme, with the inverse of the covariance matrix (Σ^{-1}) of the ensemble of parameter sets [95]. Since the eigenvectors of the Σ^{-1} matrix are identical to those of Σ, we obtained the principal components (PCs) of the ensemble of parameter sets (i.e. the eigenvectors of the covariance matrix). We then sorted the PCs in increasing order of the explained variance such that the PC with the smallest explained variance (proportional to its eigenvalue) received a rank of 1. Figure S2 (b) shows the parameters with substantial weights in these sorted eigenvectors. We note that the trends displayed by the PCs are qualitatively similar to those of the eigenvectors of the approximate Hessian in Figure S2 (b). We next examined if the eigenvectors and PCs were actually identical by studying their pairwise dot products. Figure S3 presents a heatmap of the pairwise dot products. A brighter color indicates a number closer to 1, indicating greater similarity. There is a very good correspondence between the first 8-10 eigenvectors and PCs, indicating that our iterative scheme is able to confidently estimate the stiffest directions in parameter space.

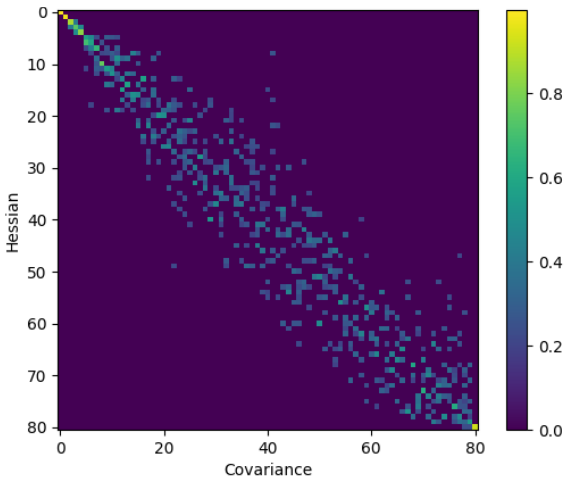

Figure S3: We compared the eigenvectors of the approximate Hessian with the principal components of the ensemble of parameter sets. The eigenvectors were sorted in descending order of their corresponding eigenvalue. The PCs were sorted in ascending order of their corresponding explained variance ratio (which is proportional to their eigenvalue). The heatmap shows the dot product of the eigenvectors and the PCs, with a brighter color implying a higher value.

S2.8 The relative ranges explored agree with the amount of data used to constrain the corresponding variable

Motivated by the success of our iterative Hessian-directed search in identifying the stiff directions of the cost function, we next examined the relationship between the stiff parameters and the data constraining the model. We first studied the relative ranges of parameter values explored for each parameter. These are visualized as ratios of parameter values with respect to $\mathbf{p}^*$ on a log10 scale in Figure S4. The parameters are sorted according to the relative ranges explored. The ensemble of parameter sets was further analyzed. The parameter ranges vary from¡ 1 to 2 orders of magnitude. Figure S4 summarizes these parameter ranges. One feature that stands out from this sorting is that the gamma parameters which govern the time scales are mostly found in the top half of the plot, with broad ranges. This is likely a consequence of the lack of time series data used to constrain most of the variables in the model. Examining the parameters with narrower ranges, at the bottom of the plot, we notice that while many parameters do occur in the equations of variables that are constrained by data, this is not the case for other parameters. Examples include ω_{cyr} (regulates basal dynamics Cyr1), $\omega_{\text{torc\_ego}}$ (regulates the stimulation of TORC1 by Gtr1/2) and ω_{gis} (regulates basal dynamics of Gis1) (Figure S4) While the ranges in the figure indicate that the model is very sloppy in general, the occurrence of these 'unconstrained' parameters at the bottom of the figure was surprising. In order to investigate the influence these parameters had on the model, we decided to carry out a detailed parameter perturbation analysis.

S2.9 Model structure exerts an important influence on the stiff/sloppy classification of parameters

In order to study the relationships among parameters, the model structure and the model constraints, we first ranked the parameters in the model by their contribution to the stiff directions. For this, an arbitrary cutoff of one standard deviation of the distribution of weights for parameters across all eigenvectors was chosen. Then, the parameters with absolute weights greater than the chosen cutoff were designated to contribute substantially to a given eigenvector. Finally, a cumulative list of parameters was constructed, where the rank of a given parameter is the eigenvector number in which it first appears with signficant weight.

From the comparison of the eigenvectors of the covariance matrix and the approximate Hessian, it can be observed that there is a good correspondence between the first 8 or 9 eigenvectors (Figure S3). These were designated the high confidence directions, and the parameters occurring in these directions are marked in bold in Table S3 respectively. A striking finding from this table is that among the top-ranked parameters,

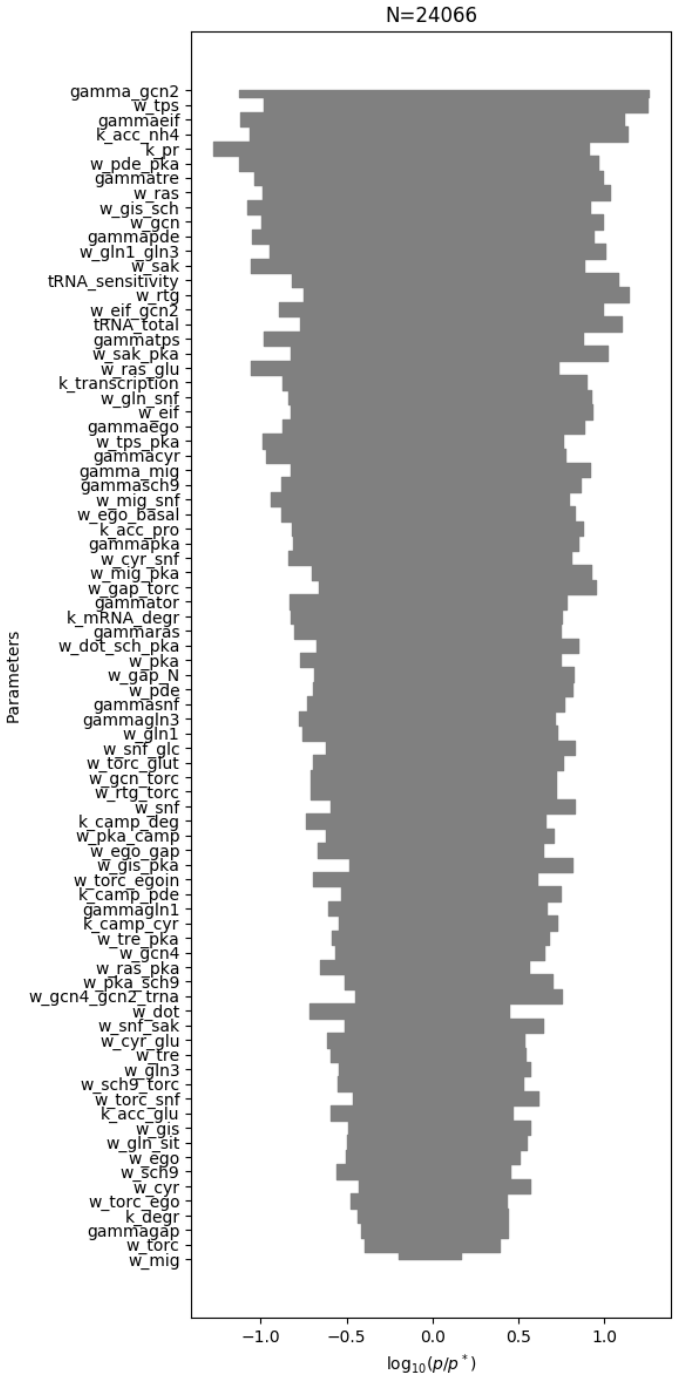

Figure S4: Ranges of parameters explored over all parameter sets at the end of four iterations. The smallest and largest value of each parameter over the ensemble were chosen, and the log10 value of the ratio with respect to the p* value was used to define the range.

many are not constrained by data, i.e., they do not appear in equations whose dynamics are constrained by data.

While the ranks of parameters in Table S3 indicate a complex relationship between model constraints and model structure influencing the structure of the cost surface, we were interested in the distribution of parameters that do appear in equations constrained by data. To investigate this distribution, starting from

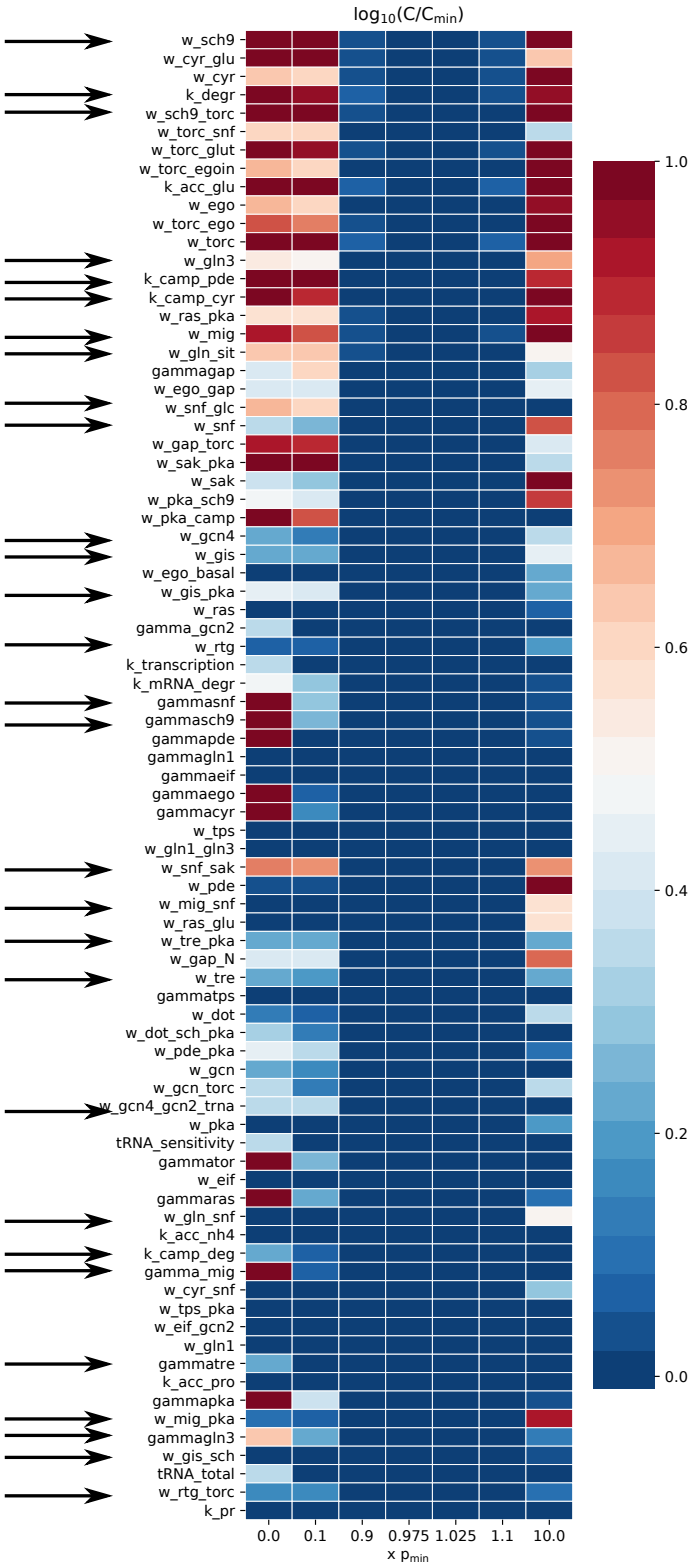

Figure S5: Parameter robustness is governed by model topology and experimental data. The arrows indicate the parameters that occur in equations constrained by data.

$\mathbf{p}^*$ we picked each parameter one at a time and perturbed its value in a ±2.5%, ±10%, and ±10-fold range and obtained the fitting cost in each instance. We also measured the model cost when the parameter was set to 0. Figure S5 shows the results of this analysis. The color of the heatmap is the log 10 fold increase in cost over $C_{\min}$. The cost values are truncated to a 10-fold increase so that smaller costs are visible. We observe that while a perturbation of up to ±10% has little effect on model cost, a 10-fold change produces a dramatic increase in model cost for the parameters on top of the ranked list, while those at the bottom of the list show a decreased effect, in agreement with the ranking of stiffness. The arrows in Figure S5 indicate the parameters which occur in equations constrained by data. We observe that these parameters do not exhibit any type of clustering, and are distributed across the entire list.

These observations indicate that, despite a small amount of data available to constrain the model, the model structure (in particular the pathway crosstalk and feedback interactions) might play an important role in indirectly constraining other parts of the model that are not directly constrained by data.

S3 Alternative interpretations of rapamycin treatment

As discussed in the section "Testing the model against observed phenotypes of mutant strains", 22 experiments that we collected from the literature relate to rapamycin treatment in various mutant strains. There are three ways of interpreting the immediate effect of rapamycin on a strain grown in rich medium. First, via the Sch9 branch of TORC1 signaling, rapamycin can lead to an inhibition of ribosome biogenesis. In our model, this would be represented as an upregulation of Dot6 activity. Second, via the Tap42-Sit4 branch of TORC1 signaling, the activities of Gln3 and Gcn4 can result in an upregulation of nitrogen starvation and adaptation responses. Finally, via mechanisms not currently present in the model, TORC1 can directly or indirectly impinge on the cell cycle machinery to cause a G1 arrest [96]. We considered the first two definitions of the effect of rapamycin on cells. As shown in Figure S6, both the Dot6 and Gln3Gcn4 definitions show a trend of decreasing median cost until 11 of 22 experiments are explained. We next describe the causes of model mismatch across both definitions of rapamycin.

Model mismatches Eleven of the 22 experiments are explained by less than 50% of the parameter sets using either definition of rapamycin treatment (Table S1). Four of the 11 rapamycin treatment experiments involve strains carrying mutations downstream of TORC1. $SCH9^{DE}$ encodes a constitutively active Sch9 kinase. *tap42-11* is a temperature senstitive allele of TAP42, which encodes a protein involved in transmitting the TORC1 signal to Sit4 and other stress response TFs. The single mutant strains $SCH9^{DE}$ and *tap42-11* are slightly resistant to rapamycin treatment, whereas the double mutant strain $SCH9^{DE}$*tap42-11* is fully resistant [97]. Using our definition of rapamycin treatment based on Gln3 and Gcn4 activities, strains involving *tap42-11* are predicted to be rapamycin resistant. However, since neither of these TFs are regulated by Sch9, the $SCH9^{DE}$ strain is predicted to be rapamycin sensitive. Additionally, three strains, namely *gln3*Δ*gat1*Δ, *gcn4*Δ, and an overexpression mutant 2μ URE2 are all predicted to be rapamycin sensitive as a consequence of our chosen definition (Sections S5.6S5.28S5.7).

Seven of the 11 rapamycin treatment experiments that we have curated include mutants of the carbon signaling pathway. These experiments clearly indicate that mutations affecting the carbon signaling pathways influence the nitrogen adaptation response, and the model's failure to explain these results give us insight into the crosstalk between carbon and nitrogen pathways. As mentioned in the description of the PKA pathway in the Results section of the main text, our model supports some results from Schmelzle *et al.*, but not from Zurita-Martinez *et al.*, originating from strain specific differences. These observations account for three of the eight mismatches ('14-bcy1', '15-ira1', and '16-ira1ira2' described in Sections S5.14S5.15S5.16). Schmelzle *et al.* examined three hyperactivating PKA strains in a *gln3*Δ*gat1*Δ background, ('19-RAS2v19gln3gat1', '20-TPK1gln3gat1', and '22-bcy1gln3gat' described in Sections S5.19S5.20S5.22). These strains were shown to be rapamycin resistant. However, our model predicts that these strains are sensitive to rapamycin. Our model does not currently include a direct interaction between PKA and TORC1. Similarly, the last rapamycin treatment mismatch relates to a *snf1*Δ strain which was observed to show rapamycin resistance [58]. While our model assumes that Snf1 inhibits TORC1, Snf1 will be inactive during growth on YPD, hence the model predicts that a *snf1* deletion will not affect Gln3 activity in this nutrient condition. Further mechanistic details of crosstalk between PKA, Snf1 and TORC1 will be needed in order to resolve these

mismatches.

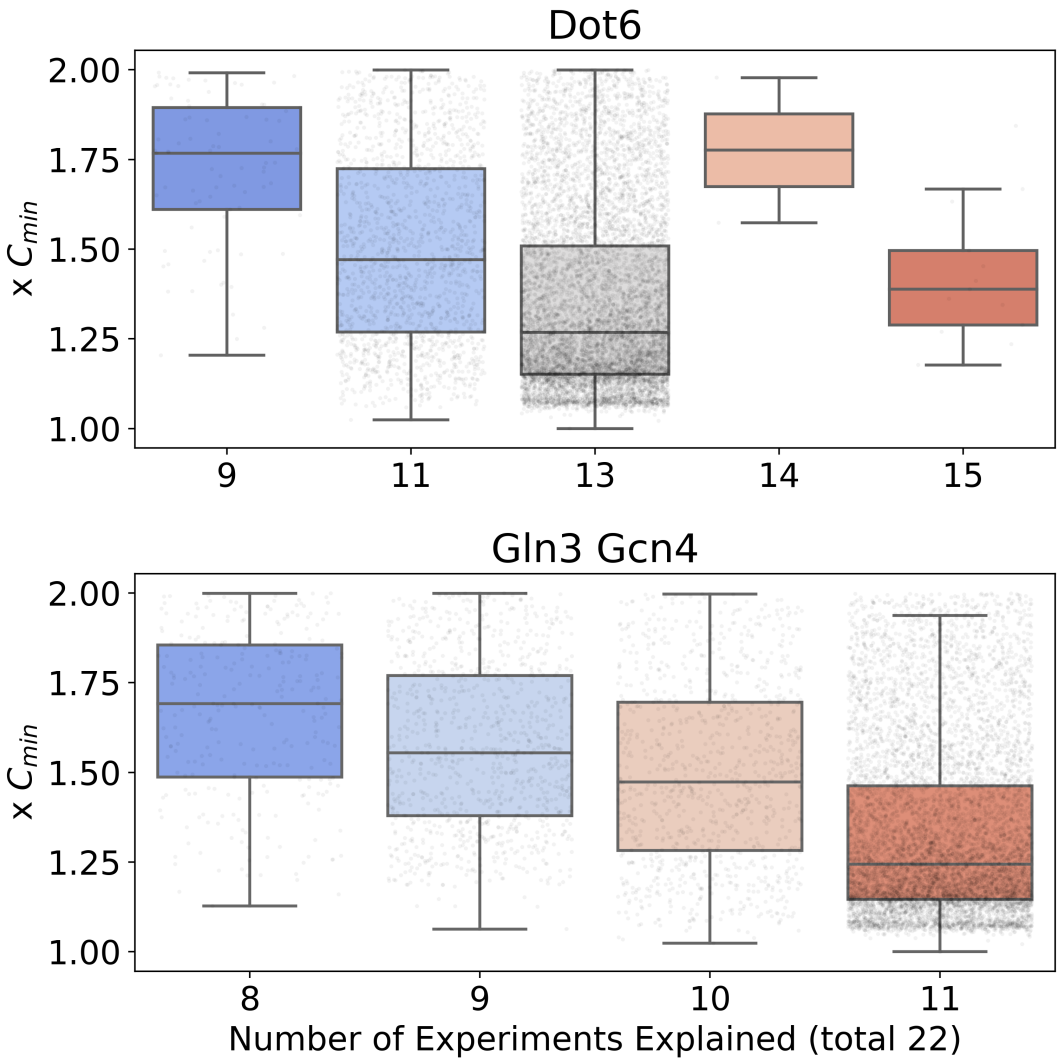

Figure S6: Dependence of model cost on explanatory capacity, across the entire collection of alternative sets of parameter values. Rapamycin experiments are defined using Dot6 as a model readout.

Exp ID	Dot6	Gln3Gcn4
20-TPK1 gln3 gat1	26.46	1.93
6-gln3 gat1	27.64	1.93
37-tap42-11	27.64	56.34
34-snf1	27.64	0.09
27-gln3 gcn4	27.64	100.0
22-bcy1 gln3 gat1	27.64	1.93
16-ira1 ira2	27.64	0.03
19-RAS2v19 gln3 gat1	27.64	1.93
14-bcy1	27.64	0.03
7-2μ URE2	27.64	1.79
15-ira1	27.64	0.03
10-gat1	72.36	83.39
9-gln3	72.36	83.39
28-gcn4	72.36	0.0
8-wt	72.36	97.25
35-reg1	72.36	98.02
36-ure2	72.36	98.07
18-tpk1	73.05	97.65
17-ras2	73.25	97.76
21-bcy1	73.54	97.96
38-SCH9^{DE}	96.66	0.63
39-SCH9^{DE} tap42	96.66	99.88

Table S1: List of rapamycin experiments, with confidence in model predictions. Confidence in qualitative predictions is expressed as the percentage of parameter sets that make the correct prediction. The *in silico* experiments corresponding to the experiment IDs are presented in Sections S5.

Name	Value
Cyr1_T	1.00e+00
Dot6_T	1.00e+00
EGO_T	1.00e+00
EGOGAP_T	1.00e+00
Gcn2_T	1.00e+00
Gcn4_T	1.00e+00
Gis1_T	1.00e+00
Gln1_T	1.00e+00
Gln3_T	1.00e+00
Mig1_T	1.00e+00
PDE_T	1.00e+00
PKA_T	1.00e+00
Ras_T	1.00e+00
Rtg13_T	1.00e+00
Sak_T	1.00e+00
Sch9_T	1.00e+00
Snf1_T	1.00e+00
TORC1_T	1.00e+00
Tps1_T	1.00e+00
Trehalase_T	1.00e+00
eIF_T	1.00e+00
gamma_gcn2	4.71e+00
gamma_mig	6.56e-01
gammacyr	8.96e+00
gammaego	5.07e+01
gammaeif	4.71e-01
gammagap	5.62e-01
gammagln1	6.35e-02
gammagln3	8.09e-02
gammapde	2.82e-01
gammapka	2.68e+00
gammaras	1.82e+00
gammasch9	4.63e+00
gammasnf	8.20e-01
gammator	7.55e+00
gammatps	4.71e-01
gammatre	3.42e-01
k_acc_glu	4.92e-02
k_acc_nh4	1.47e-03
k_acc_pro	2.15e-04
k_camp_cyr	1.09e+01
k_camp_deg	8.38e-02
k_camp_pde	1.41e+01

Name	Value
k_degr	8.98e-02
k_mRNA_degr	7.30e-02
k_pr	2.02e-02
k_transcription	2.36e-01
sigma_cyr	3.50e+00
sigma_dot	2.00e+01
sigma_ego	5.00e+00
sigma_eif	1.00e+00
sigma_gap	1.00e+00
sigma_gcn2	2.00e+01
sigma_gcn4	5.00e+00
sigma_gis1	1.00e+01
sigma_gln	1.00e+01
sigma_gln1	1.00e+00
sigma_mig1	2.70e-01
sigma_pde	1.90e+00
sigma_pka	1.00e+00
sigma_ras	1.00e+00
sigma_rtg	1.00e+01
sigma_sak	2.00e+01
sigma_sch9	8.00e+00
sigma_snf	3.00e+00
sigma_tor	5.00e+00
sigma_tps	5.00e+00
sigma_trehalase	1.00e+01
tRNA_scale	7.45e+01
tRNA_total	2.47e+00
w_cyr	1.35e+00
w_cyr_glu	5.13e+00
w_cyr_snf	1.19e-01
w_dot	2.93e-01
w_dot_sch_pka	1.63e-01
w_ego	2.84e-01
w_ego_basal	1.10e-02
w_ego_gap	2.21e+00
w_eif	3.73e+00
w_eif_gcn2	2.76e-01
w_gap_N	7.76e+00
w_gap_torc	8.83e+01
w_gcn	1.15e-01
w_gcn_torc	1.29e+00
w_gcn4	7.43e-01
w_gcn4_gcn2_trna	1.53e+00

Name	Value
w_gis	1.30e+00
w_gis_pka	3.30e+00
w_gis_sch	8.42e-01
w_gln_sit	8.61e-01
w_gln_snf	3.90e+00
w_gln1	2.22e-01
w_gln1_gln3	5.20e-01
w_gln3	6.39e-01
w_mig	1.06e+01
w_mig_pka	2.31e+00
w_mig_snf	1.21e+00
w_pde	3.83e-01
w_pde_pka	2.89e+00
w_pka	5.81e-02
w_pka_camp	1.02e+02
w_pka_sch9	1.75e+01
w_ras	2.08e-02
w_ras_glu	2.07e-01
w_ras_pka	1.87e+00
w_rtg	1.86e-01
w_rtg_torc	8.77e-01
w_sak	2.05e-01
w_sak_pka	3.75e-01
w_sch9	5.65e-01
w_sch9_torc	1.96e+00
w_snf	5.38e-01
w_snf_glc	1.15e+00
w_snf_sak	1.52e+00
w_torc	5.39e-01
w_torc_ego	8.77e-01
w_torc_egoin	3.03e-01
w_torc_glut	8.63e-01
w_torc_snf	4.37e-01
w_tps	5.30e-02
w_tps_pka	5.74e-01
w_tre	1.07e+00
w_tre_pka	3.07e+00
ATP	1.0
Carbon	1.0
Glutamine_ext	1.0
NH4	0.00e+00
Proline	0.00e+00

Table S2: Parameter values constituting the optimal parameter set, obtained from 10,000 steps of MCMC sampling. This set of values is used to define the simulation of a *wt* strain under HCHN conditions. Four time scale parameters describing the activation of transcription factors namely $\gamma_{gcn4}, \gamma_{rtg13}, \gamma_{gis1}, \gamma_{dot6}$ are set to 1, since there is no short time scale data available to constrain their dynamics.

Index	Parameter	Ranks	Data?	Index	Parameter	Ranks	Data?
1	**w_sch9**	1	Yes (T,P)	42	**gammaego**	8	No
2	**w_cyr_glu**	1	No	43	**gammacyr**	8	No
3	**w_cyr**	1	No	44	**w_tps**	8	No
4	**k_degr**	1	Yes (T,P)	45	**w_gln1_gln3**	8	No
5	**w_sch9_torc**	1	Yes (T,P)	46	**w_snf_sak**	9	Yes (T,P)
6	**w_torc_snf**	1	No	47	**w_pde**	9	No
7	**w_torc_glut**	1	No	48	**w_mig_snf**	9	Yes (T)
8	**w_torc_egoin**	1	No	49	**w_ras_glu**	9	No
9	**k_acc_glu**	1	No	50	**w_tre_pka**	9	Yes (P)
10	**w_ego**	1	No	51	**w_gap_N**	9	No
11	**w_torc_ego**	1	No	52	**w_tre**	9	Yes (P)
12	**w_torc**	1	No	53	**w_gcn**	10	No
13	**w_gln3**	2	Yes (T,P)	54	**w_dot**	10	No
14	**k_camp_pde**	2	Yes (T,P)	55	**gammatps**	10	No
15	**k_camp_cyr**	2	Yes (T,P)	56	**w_pde_pka**	10	No
16	**w_ras_pka**	2	No	57	**w_dot_sch_pka**	10	No
17	**w_mig**	2	Yes (T,P)	58	**w_gcn_torc**	10	No
18	**w_gln_sit**	3	Yes (T,P)	59	**w_gcn4_gcn2_trna**	10	Yes (P)
19	**gammagap**	4	No	60	w_pka	11	No
20	**w_ego_gap**	4	No	61	k_acc_nh4	11	No
21	**w_snf_glc**	6	Yes (T,P)	62	gammaras	11	No
22	**w_snf**	6	Yes (T,P)	63	k_camp_deg	11	Yes (T,P)
23	**w_gap_torc**	6	No	64	tRNA_sensitivity	11	No
24	**w_sak_pka**	6	No	65	gammator	11	No
25	**w_sak**	6	No	66	w_gln_snf	11	Yes (T,P)
26	**w_pka_sch9**	6	No	67	w_eif	11	No
27	**w_pka_camp**	7	No	68	gamma_mig	11	Yes (T)
28	**w_gcn4**	8	Yes (P)	69	w_cyr_snf	12	No
29	**w_gis**	8	Yes (P)	70	w_eif_gcn2	12	No
30	**w_ego_basal**	8	No	71	w_tps_pka	12	No
31	**w_gis_pka**	8	Yes (P)	72	w_gln1	12	No
32	**w_ras**	8	No	73	gammatre	13	Yes (P)
33	**gamma_gcn2**	8	No	74	gammagln3	14	Yes (T,P)
34	**w_rtg**	8	Yes (P)	75	w_gis_sch	14	Yes (P)
35	**k_transcription**	8	No	76	k_acc_pro	14	No
36	**k_mRNA_degr**	8	No	77	tRNA_total	14	No
37	**gammasnf**	8	Yes (T,P)	78	gammapka	16	No
38	**gammasch9**	8	Yes (T,P)	79	w_mig_pka	16	Yes (T)
39	**gammapde**	8	No	80	w_rtg_torc	18	Yes (P)
40	**gammagln1**	8	No	81	k_pr	20	No
41	**gammaeif**	8	No				

Table S3: Ranked list of parameters. The 'Data?' column indicates whether or not the equation in which a parameter appears is contrained by any type of data. If it is constrained, the column further indicates the type of data, 'T' for timecourses or 'P' for perturbations. The parameters highlighted in bold indicate those appearing in the first 10 stiff directions.

Strain	Model definition	Description
Δsch9	Sch9_T = 0	Total amount of model variable
Δtor1	TORC1_T = 0	Total amount of model variable
Δsnf1	Snf1_T = 0	Total amount of model variable
Δgtr1/2	EGO_T = 0	Total amount of model variable
Δpde1/2	PDE_T = 0	Total amount of model variable
Δlst4/7	EGOGAP_T = 0	Total amount of model variable
Δras2	Ras_T = 0	Total amount of model variable
Δsak1	Sak_T = 0	Total amount of model variable
Δgcn2	Gcn2_T = 0	Total amount of model variable
Δcyr1	Cyr1_T = 0	Total amount of model variable
Δtpk1/2/3	PKA_T = 0	Total amount of model variable
GCN2-S557	w_gcn_torc = 0	TORC1 regulation of Gcn2
GLN3 ΔST	w_gln_snf = 0	Snf1 regulation of Gln3
GLN3 ΔTT	w_gln_sit = 0	TORC1 regulation of Gln3
Δbcy1	w_pka_sch9 = 0	Bcy1 mediated downregulation of PKA by Sch9
Δira1/2	w_ras_pka = 0	Ira1/2 mediated downregulation of Ras2 by PKA

Table S4: Summary of model representation of 16 mutants investigated in Section 'Predictions of global cellular responses to nutrient states'. The columns represent the strain, the parameter change used to represent the strain in the model, and an interpretation of the parameter in the context of the model, respectively.

S4 Steady-state and time-course predictions

In Figure 4 we presented global transcription factor states in response to complex nutrient shifts in 16 mutant strains and *wt*. 11 out of 16 mutant strains correspond to deletions of molecular species present in the model (Sch9, TORC1, Snf1, Gtr1/2, EGOGAP (Lst4/7), PDE, Ras2, Sak1, Gcn2, Cyr1, PKA). The remaining 5 mutant strains do not correspond directly to model variables. Δbcy1 and Δira1/2 correspond to molecular species implicitly represented by regulatory interactions in our model. GCN2-S557, GLN3 ΔST, and GLN3 ΔTT represent mutant strains that abolish some but not all regulatory interactions impinging on targets, namely the Gcn2 kinase and the Gln3 transcription factor respectively. Table S4 summarizes how the 16 strains are represented in the model.

This section includes supplementary results that quantify the robustness of the model. Figure S5 is an alternate presentation of Figure 4. Each cell in the table records the percentage of parameter sets that agree that a given TF is ON in a given strain (defined by the row), in a given nutrient condition (defined by the column).

In addition to Figure 4, which depicts the robustness of the steady state responses of key transcription factors, we also investigated the robustness of the time-course predictions made by the model in Figure S8S9S10S11, which show the predicted time-courses of four prominent variables in the model, Snf1, Sch9, PKA, and cAMP. One hundred randomly sampled parameter sets were used to simulate the responses of these variables in various strains (rows) in various nutrient conditions (columns). Further, we quantified the deviation of these time-courses from those predicted by the optimal parameter set using the mean sum of squared errors (MSE). We defined a parameter set to be robust for that prediction, if the time-course deviation was less than the an assigned cutoff on the MSE. Figure S7 summarizes the robustness of time-course predictions, following the same color conventions as Figure 4.

Figure S7: Robust time courses of Snf1, Sch9, PKA, and cAMP across the indicated strains in the 8 qualitatively distinct nutrient states. The figure summarizes the deviation of simulated trajectories across 500 randomly sampled parameter sets with respect to that from the reference parameter set. We use mean sum of squared errors (MSE) to measure the deviation. Green and red bars indicate the fraction of parameter sets with MSE less than and greater than a chosen cutoff respectively. Light colors indicate robust timecourse, with greater than 90% of the parameter sets producing MSE less than a cutoff. Conversely, bright colors indicate fragile predictions with more than 10% of parameter sets making fragile predictions.

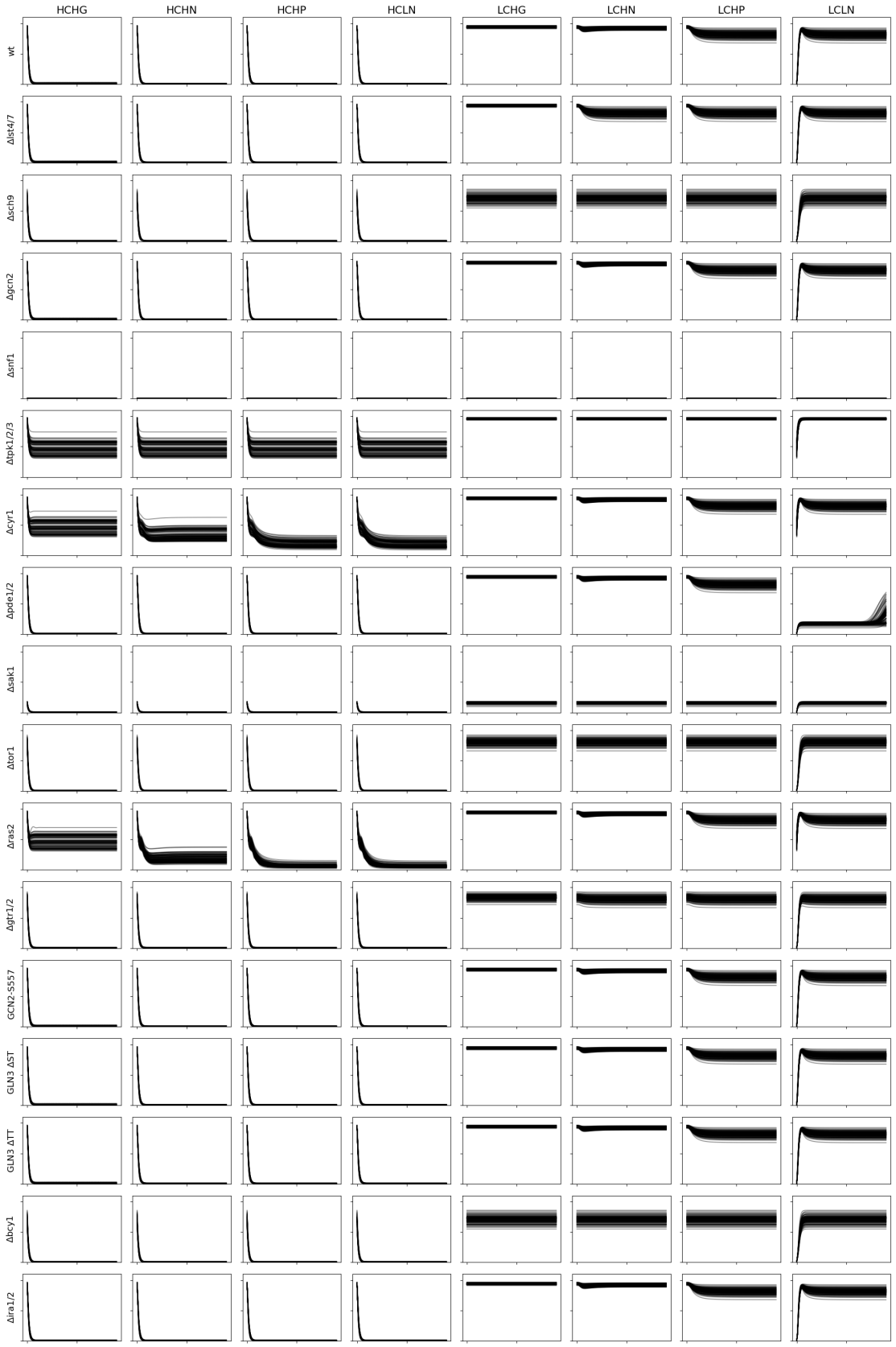

Figure S8: Snf1 dynamics across 100 randomly sampled parameter sets.

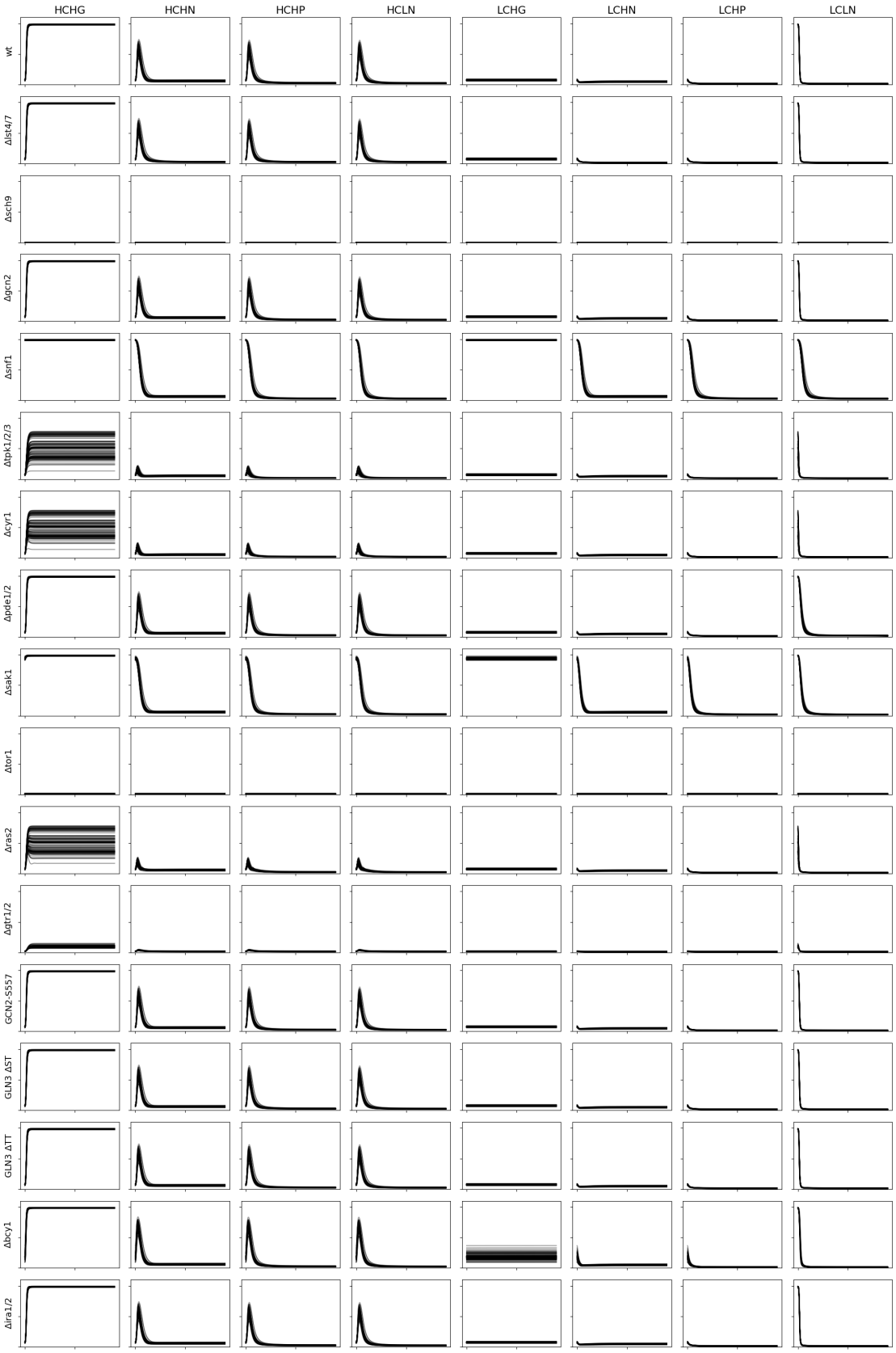

Figure S9: Sch9 dynamics across 100 randomly sampled parameter sets.

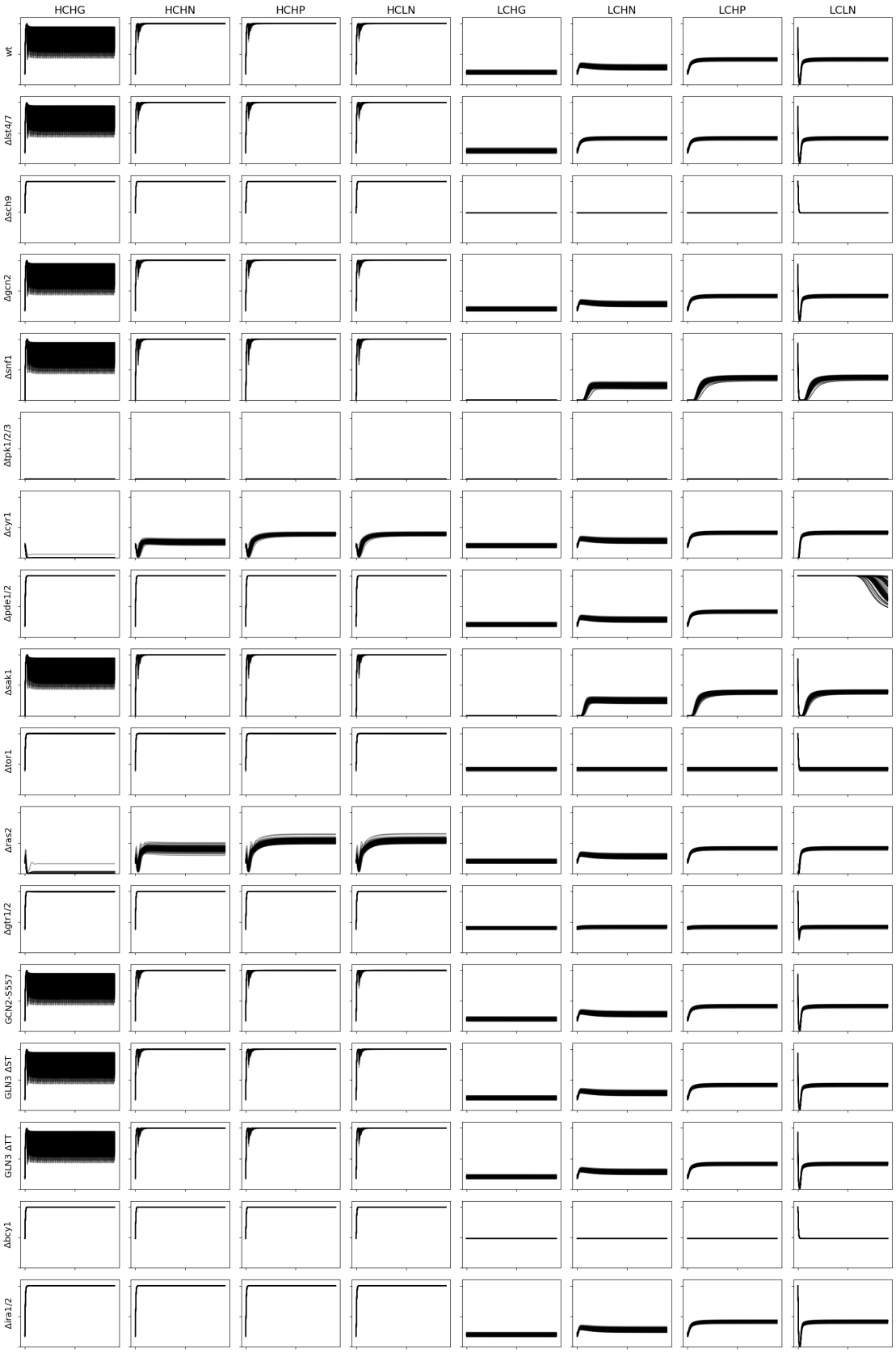

Figure S10: PKA dynamics across 100 randomly sampled parameter sets.

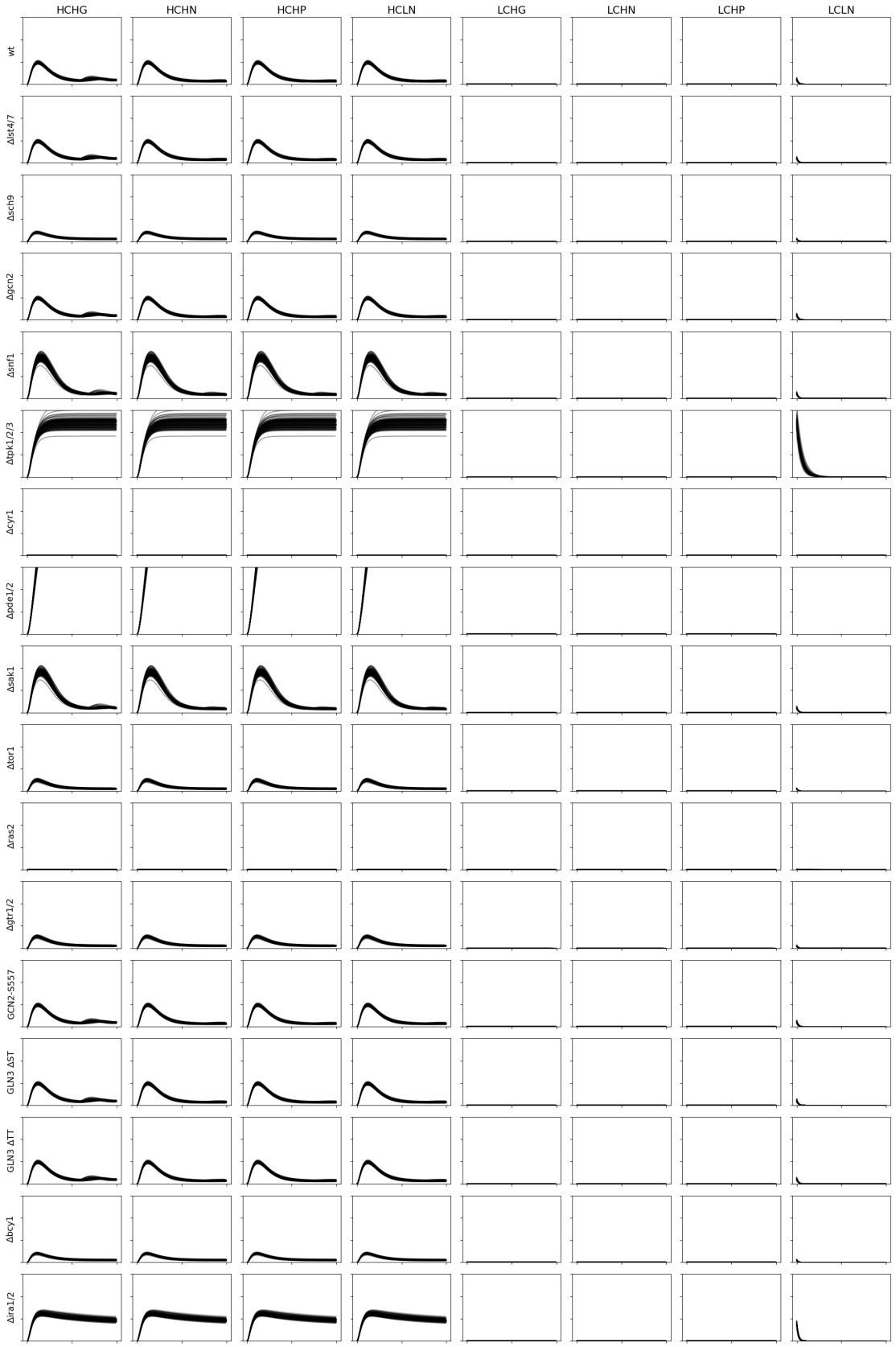

Figure S11: cAMP dynamics across 100 randomly sampled parameter sets.

S5 Comparison of model predictions with qualitative experimental data

This section records the curated qualitative experiments, along with the model simulations using the optimal parameter set. Each experiment has a unique experiment ID, a table containing the interpreted and predicted states of transcription factors, along with the simulated values at steady state, a description of the experiment containing a reference to the original publication, the strain used, and the experiment performed, and the parameters used to represent the strain and the shift experiment in the model. Finally, the simulated time courses of the six model readouts and the interpretation of the simulation are described.

As described in Section S3, we use two definitions of rapamycin experiments. The sample simulations here use the Gln3Gcn4 definition of rapamycin treatment. Experiments involving rapamycin treatment are thus indicated using the text **Readout used is Gln3 Gcn4**. For the general trend of predictions using the alternate definition using Dot6, please see Table S1. (Note that the results shown here only correspond to one parameter set of our collection of 18,000 alternate sets of parameter values.)

S5.1 1-rho0

TF	Interpreted	Simulated	Simulation
Gis1	-	-	0.000
Mig1	-	-	1.487
Dot6	-	-	0.312
Gcn4	-	-	0.024
Rtg13	Off	Off	0.274
Gln3	-	-	0.983

Description: Liu et al, 1999 studied a *rho0* strain (PSY142 ρ^0) grown in YP + 5% glucose.
Representation:

Preshift Parameters

ATP	0.1
Carbon	0.1
$\text{Glutamine}_{\text{ext}}$	1.0

Postshift Parameters

ATP	1.0
Carbon	1.0
$\text{Glutamine}_{\text{ext}}$	1.0

Postshift Initial Conditions

Mutant definition

Parameters

k_{accglu}	0.0369
k_{accpro}	0.0002
k_{accnh4}	0.0011

Initial conditions

Model agrees with experiment.

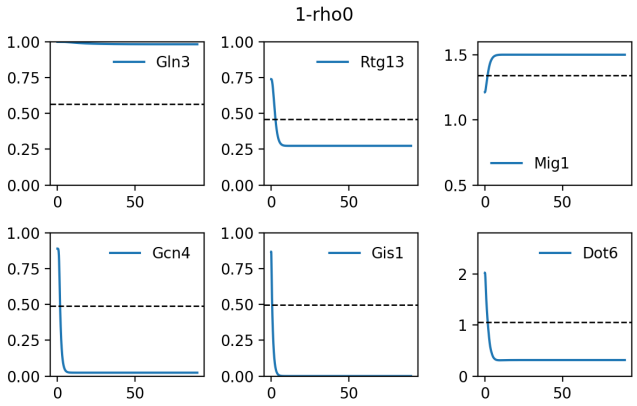

S5.2 2-rho0

TF	Interpreted	Simulated	Simulation
Gis1	-	-	0.000
Mig1	-	-	1.482
Dot6	-	-	1.121
Gcn4	-	-	0.722
Rtg13	On	On	0.683
Gln3	-	-	0.999

Description: Liu et al, 1999 studied a *rho0* strain (PSY142 ρ^0) grown in YP + 2% raffinose.
Representation:

Preshift Parameters		*Postshift Parameters*		*Postshift Initial Conditions*
ATP	0.1	ATP	0.7	
Carbon	0.1	Carbon	0.7	
$\text{Glutamine}_{\text{ext}}$	1.0	$\text{Glutamine}_{\text{ext}}$	0.5	

Mutant definition

Parameters		*Initial conditions*
k_{accglu}	0.0369	
k_{accpro}	0.0002	
k_{accnh4}	0.0011	

Model agrees with experiment.

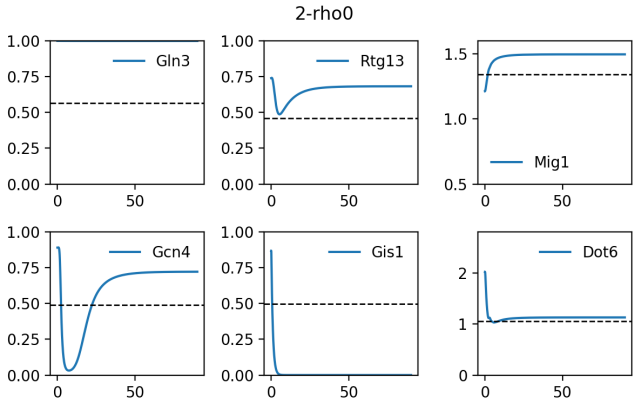

S5.3 3-rtg1

TF	Interpreted	Simulated	Simulation
Gis1	-	-	0.000
Mig1	-	-	1.498
Dot6	-	-	0.532
Gcn4	-	-	0.024
Rtg13	Off	Off	0.279
Gln3	-	-	0.992

Description: Liu et al, 1999 studied a *rtg1* strain (PSY142 ρ^0) grown in YNBD + 0.02% Glutamate.
Representation:

Preshift Parameters		*Postshift Parameters*		*Postshift Initial Conditions*
ATP	1.0	ATP	1.0	
Carbon	1.0	Carbon	1.0	
$\text{Glutamine}_{\text{ext}}$	1.0	$\text{Glutamine}_{\text{ext}}$	0.9	

Mutant definition

Parameters

$Rtg13_T$	0.75
k_{accglu}	0.0369
k_{accpro}	0.0002
k_{accnh4}	0.0011

Initial conditions

Model agrees with experiment.

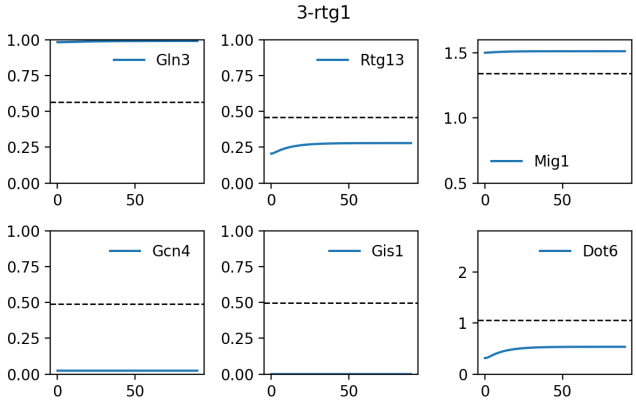

S5.4 4-rtg1

TF	Interpreted	Simulated	Simulation
Gis1	-	-	0.000
Mig1	-	-	1.503
Dot6	-	-	1.094
Gcn4	-	-	0.945
Rtg13	Off	On	0.613
Gln3	-	-	1.000

Description: Liu et al, 1999 studied a *rtg1* strain (PSY142 ρ^0) grown in YNBD.

Representation:

Preshift Parameters

ATP	1.0
Carbon	1.0
$Glutamine_{ext}$	1.0

Postshift Parameters

ATP	1.0
Carbon	1.0
$Glutamine_{ext}$	0.0

Postshift Initial Conditions

Mutant definition

Parameters

$Rtg13_T$	0.75
k_{accglu}	0.0369
k_{accpro}	0.0002
k_{accnh4}	0.0011

Initial conditions

Model does not agree with experiment.

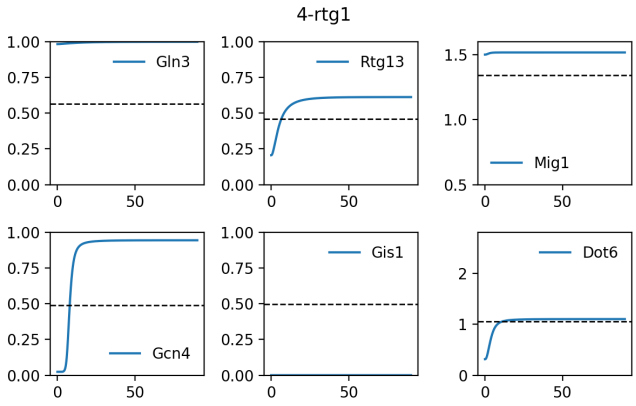

S5.5 5-snf1

TF	Interpreted	Simulated	Simulation
Gis1	Off	On	0.884
Mig1	On	Off	1.325
Dot6	-	-	1.977
Gcn4	-	-	0.872
Rtg13	-	-	0.728
Gln3	-	-	0.999

Description: Gasmi et al, 2014 studied a *snf1* strain (BY4741) grown in Minimal + (0.2%casa) + 2% Ethanol.

Representation:

Preshift Parameters

ATP	1.0
Carbon	1.0
$\text{Glutamine}_{\text{ext}}$	1.0

Postshift Parameters

ATP	0.1
Carbon	0.1
$\text{Glutamine}_{\text{ext}}$	0.2

Postshift Initial Conditions

Mutant definition

Parameters

Snf1_{T}	0.0

Initial conditions

Snf1	0.0

Model does not agree with experiment.

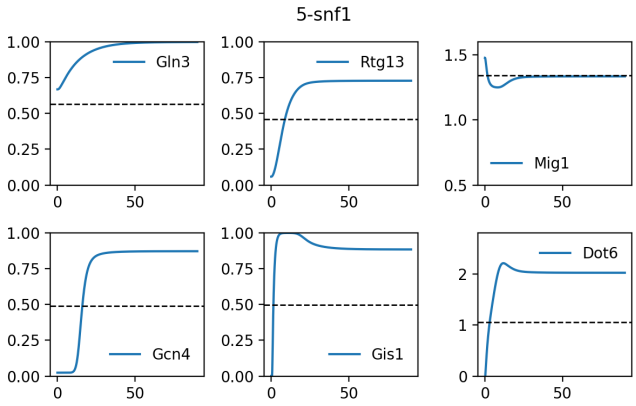

S5.6 6-gln3 gat1

Readout used is Gln3 Gcn4

TF	Interpreted	Simulated	Simulation
Gis1	-	-	0.000
Mig1	-	-	1.503
Dot6	-	-	1.108
Gcn4	Off	On	0.955
Rtg13	-	-	0.866
Gln3	Off	Off	0.000

Description: Beck et al, 1999 studied a *gln3 gat1* strain (wt) grown in YPD + rapamycin.
Representation:

Preshift Parameters

ATP	1.0
Carbon	1.0
$\text{Glutamine}_{\text{ext}}$	1.0

Postshift Parameters

ATP	1.0
Carbon	1.0
$\text{Glutamine}_{\text{ext}}$	1.0
TORC1_{T}	0.0

Postshift Initial Conditions

TORC1	0

Mutant definition

Parameters

Gln3_{T}	0.0

Initial conditions

Gln3	0.0

Model does not agree with experiment.

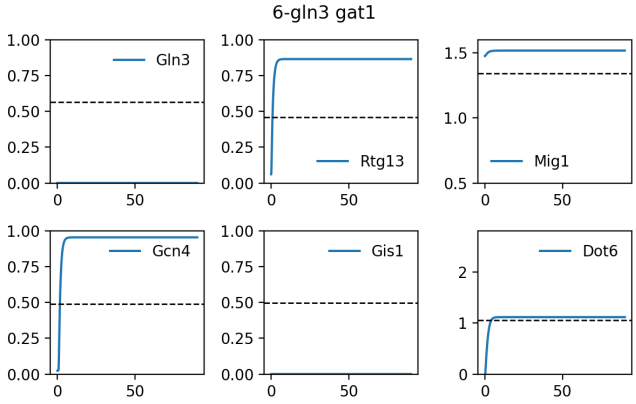

S5.7 7-2μ URE2

Readout used is Gln3 Gcn4

TF	Interpreted	Simulated	Simulation
Gis1	-	-	0.000
Mig1	-	-	1.503
Dot6	-	-	1.108
Gcn4	Off	On	0.955
Rtg13	-	-	0.866
Gln3	Off	On	0.999

Description: Beck et al, 1999 studied a *2μ URE2* strain (wt) grown in YPD + rapamycin.
Representation:

Preshift Parameters

ATP	1.0
Carbon	1.0
$\text{Glutamine}_{\text{ext}}$	1.0

Postshift Parameters

ATP	1.0
Carbon	1.0
$\text{Glutamine}_{\text{ext}}$	1.0
TORC1_{T}	0.0

Postshift Initial Conditions

TORC1	0

Mutant definition

Parameters

w_{gln3}	1.2784

Initial conditions

Model does not agree with experiment.

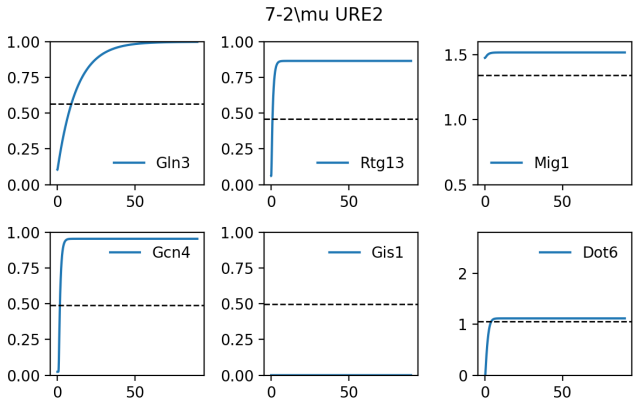

S5.8 8-wt

Readout used is Gln3 Gcn4

TF	Interpreted	Simulated	Simulation
Gis1	-	-	0.000
Mig1	-	-	1.503
Dot6	-	-	1.108
Gcn4	On	On	0.955
Rtg13	-	-	0.866
Gln3	On	On	1.000

Description: Beck et al, 1999 studied a *wt* strain (wt) grown in YPD + rapamycin.
Representation:

Preshift Parameters

ATP	1.0
Carbon	1.0
$\text{Glutamine}_{\text{ext}}$	1.0

Postshift Parameters

ATP	1.0
Carbon	1.0
$\text{Glutamine}_{\text{ext}}$	1.0
TORC1_{T}	0.0

Postshift Initial Conditions

TORC1	0

Mutant definition
Parameters *Initial conditions*
Model agrees with experiment.

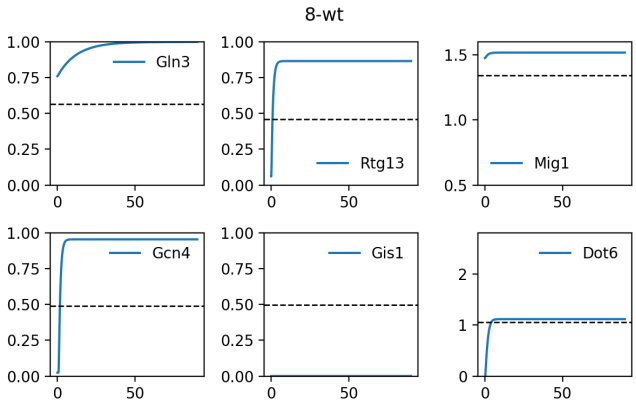

S5.9 9-gln3

Readout used is Gln3 Gcn4

TF	Interpreted	Simulated	Simulation
Gis1	-	-	0.000
Mig1	-	-	1.503
Dot6	-	-	1.108
Gcn4	On	On	0.955
Rtg13	-	-	0.866
Gln3	On	On	0.650

Description: Beck et al, 1999 studied a *gln3* strain (wt) grown in YPD + rapamycin.
Representation:

Preshift Parameters

ATP	1.0
Carbon	1.0
$\text{Glutamine}_{\text{ext}}$	1.0

Postshift Parameters

ATP	1.0
Carbon	1.0
$\text{Glutamine}_{\text{ext}}$	1.0
TORC1_{T}	0.0

Postshift Initial Conditions

TORC1	0

Mutant definition

Parameters

Gln3_{T}	0.65

Initial conditions

Gln3	0.0

Model agrees with experiment.

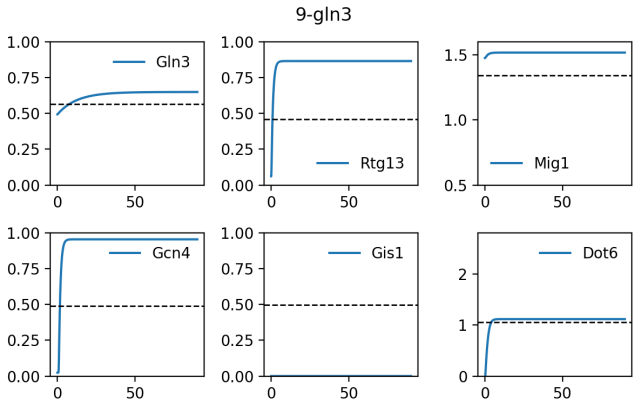

S5.10 10-gat1

Readout used is Gln3 Gcn4

TF	Interpreted	Simulated	Simulation
Gis1	-	-	0.000
Mig1	-	-	1.503
Dot6	-	-	1.108
Gcn4	On	On	0.955
Rtg13	-	-	0.866
Gln3	On	On	0.650

Description: Beck et al, 1999 studied a *gat1* strain (wt) grown in YPD + rapamycin.
Representation:

Preshift Parameters

ATP	1.0
Carbon	1.0
$\text{Glutamine}_{\text{ext}}$	1.0

Postshift Parameters

ATP	1.0
Carbon	1.0
$\text{Glutamine}_{\text{ext}}$	1.0
TORC1_{T}	0.0

Postshift Initial Conditions

TORC1	0

Mutant definition

Parameters

Gln3_{T}	0.65

Initial conditions

Gln3	0.0

Model agrees with experiment.

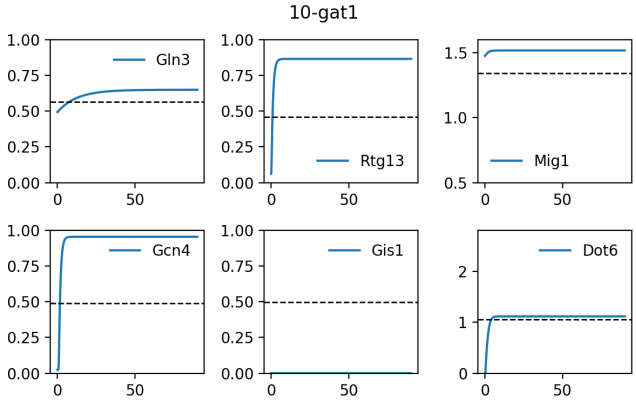

S5.11 11-gln3

TF	Interpreted	Simulated	Simulation
Gis1	-	-	0.000
Mig1	-	-	1.503
Dot6	-	-	1.037
Gcn4	-	-	0.806
Rtg13	-	-	0.702
Gln3	Off	On	0.649

Description: Crespo et al, 2002 studied a *gln3* strain (TB123) grown in SD + 1mM MSX.
Representation:

Preshift Parameters

ATP	1.0
Carbon	1.0
$\text{Glutamine}_{\text{ext}}$	1.0

Postshift Parameters

ATP	1.0
Carbon	1.0
$\text{Glutamine}_{\text{ext}}$	1.0
k_{accglu}	0.0

Postshift Initial Conditions

Mutant definition

Parameters

Gln3_{T}	0.65

Initial conditions

Gln3	0.0
Glutamine	0.01

Model does not agree with experiment.

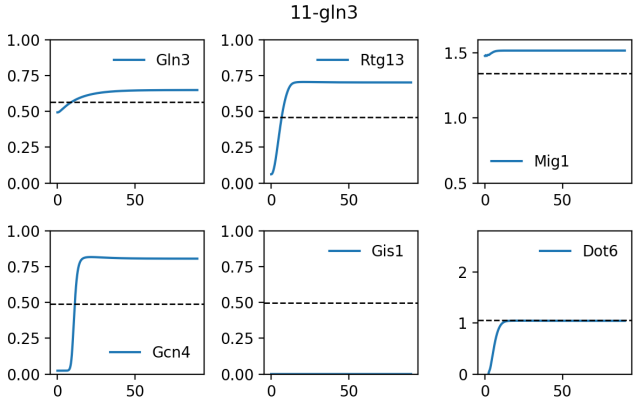

S5.12 12-gln3 gat1

TF	Interpreted	Simulated	Simulation
Gis1	-	-	0.000
Mig1	-	-	1.503
Dot6	-	-	1.037
Gcn4	-	-	0.806
Rtg13	-	-	0.702
Gln3	Off	Off	0.000

Description: Crespo et al, 2002 studied a *gln3 gat1* strain (TB123) grown in SD + 1mM MSX.
Representation:

Preshift Parameters

ATP	1.0
Carbon	1.0
$\text{Glutamine}_{\text{ext}}$	1.0

Postshift Parameters

ATP	1.0
Carbon	1.0
$\text{Glutamine}_{\text{ext}}$	1.0
k_{accglu}	0.0

Postshift Initial Conditions

Mutant definition

Parameters

Gln3_{T}	0.0

Initial conditions

Gln3	0.0
Glutamine	0.01

Model agrees with experiment.

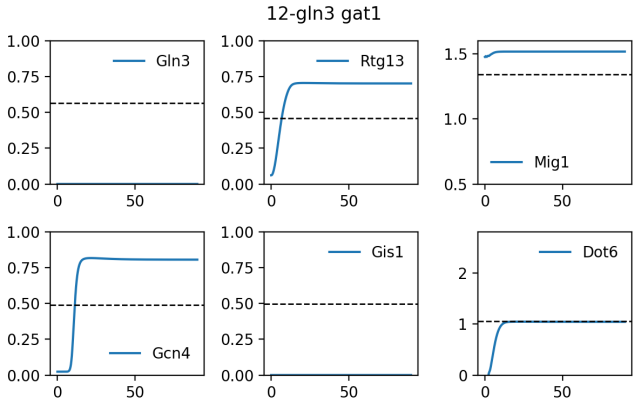

S5.13 13-wt

TF	Interpreted	Simulated	Simulation
Gis1	-	-	0.000
Mig1	-	-	1.503
Dot6	-	-	1.037
Gcn4	-	-	0.806
Rtg13	-	-	0.702
Gln3	On	On	0.999

Description: Crespo et al, 2002 studied a *wt* strain (TB123) grown in SD + 1mM MSX.
Representation:

Preshift Parameters

ATP	1.0
Carbon	1.0
$\text{Glutamine}_{\text{ext}}$	1.0

Postshift Parameters

ATP	1.0
Carbon	1.0
$\text{Glutamine}_{\text{ext}}$	1.0
k_{accglu}	0.0

Postshift Initial Conditions

Mutant definition

Parameters

Initial conditions

Model agrees with experiment.

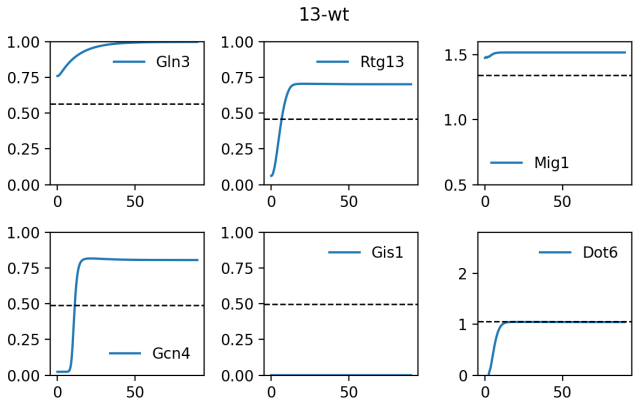

S5.14 14-bcy1

Readout used is Gln3 Gcn4

TF	Interpreted	Simulated	Simulation
Gis1	-	-	0.000
Mig1	-	-	1.503
Dot6	-	-	1.108
Gcn4	Off	On	0.955
Rtg13	-	-	0.866
Gln3	Off	On	1.000

Description: Zurita-Martinez et al, 2005 studied a *bcy1* strain (S1278b) grown in YP Glucose + 50nM rapamycin.

Representation:

Preshift Parameters

ATP	1.0
Carbon	1.0
$\text{Glutamine}_{\text{ext}}$	1.0

Postshift Parameters

ATP	1.0
Carbon	1.0
$\text{Glutamine}_{\text{ext}}$	1.0
TORC1_{T}	0.0

Postshift Initial Conditions

TORC1	0

Mutant definition

Parameters

w_{pkasch9}	0.0

Initial conditions

Model does not agree with experiment.

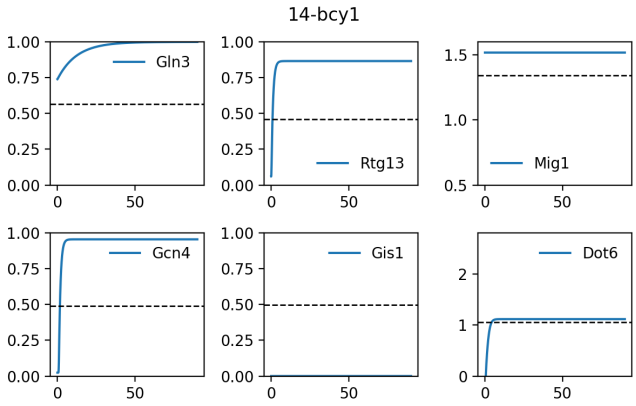

S5.15 15-ira1

Readout used is Gln3 Gcn4

TF	Interpreted	Simulated	Simulation
Gis1	-	-	0.000
Mig1	-	-	1.503
Dot6	-	-	1.108
Gcn4	Off	On	0.955
Rtg13	-	-	0.866
Gln3	Off	On	1.000

Description: Zurita-Martinez et al, 2005 studied a *ira1* strain (S1278b) grown in YP Glucose + 50nM rapamycin.

Representation:

Preshift Parameters

ATP	1.0
Carbon	1.0
$\text{Glutamine}_{\text{ext}}$	1.0

Postshift Parameters

ATP	1.0
Carbon	1.0
$\text{Glutamine}_{\text{ext}}$	1.0
TORC1_{T}	0.0

Postshift Initial Conditions

TORC1	0

Mutant definition

Parameters

w_{raspka}	0.9362

Initial conditions

Model does not agree with experiment.

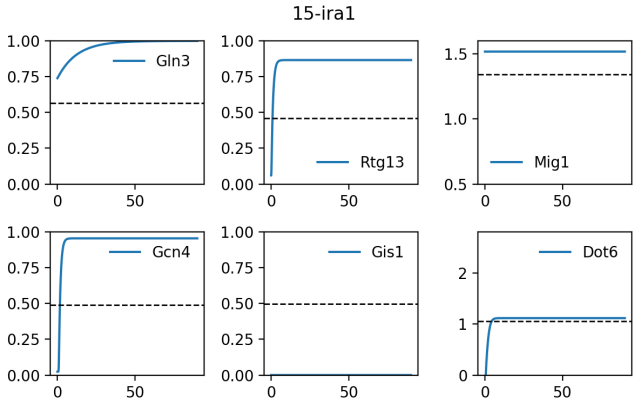

S5.16 16-ira1 ira2

Readout used is Gln3 Gcn4

TF	Interpreted	Simulated	Simulation
Gis1	-	-	0.000
Mig1	-	-	1.503
Dot6	-	-	1.108
Gcn4	Off	On	0.955
Rtg13	-	-	0.866
Gln3	Off	On	1.000

Description: Zurita-Martinez et al, 2005 studied a *ira1 ira2* strain (S1278b) grown in YP Glucose + 50nM rapamycin.

Representation:

Preshift Parameters

ATP	1.0
Carbon	1.0
$\text{Glutamine}_{\text{ext}}$	1.0

Postshift Parameters

ATP	1.0
Carbon	1.0
$\text{Glutamine}_{\text{ext}}$	1.0
TORC1_{T}	0.0

Postshift Initial Conditions

TORC1	0

Mutant definition

Parameters

w_{raspka}	0.1872

Initial conditions

Model does not agree with experiment.

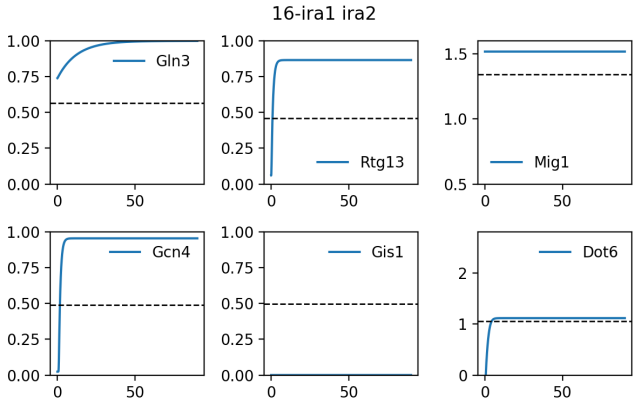

S5.17 17-ras2

Readout used is Gln3 Gcn4

TF	Interpreted	Simulated	Simulation
Gis1	-	-	0.001
Mig1	-	-	1.399
Dot6	-	-	1.637
Gcn4	On	On	0.955
Rtg13	-	-	0.866
Gln3	On	On	1.000

Description: Zurita-Martinez et al, 2005 studied a *ras2* strain (MLY41a) grown in YP Glucose + 50nM rapamycin.

Representation:

Preshift Parameters

ATP	1.0
Carbon	1.0
$\text{Glutamine}_{\text{ext}}$	1.0

Postshift Parameters

ATP	1.0
Carbon	1.0
$\text{Glutamine}_{\text{ext}}$	1.0
TORC1_{T}	0.0

Postshift Initial Conditions

TORC1	0

Mutant definition

Parameters

Ras_{T}	0.0

Initial conditions

Model agrees with experiment.

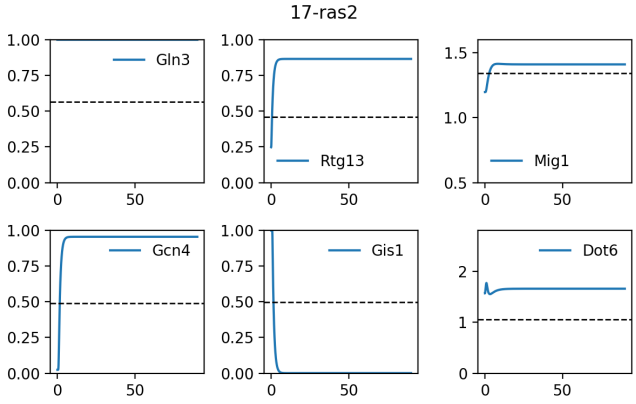

S5.18 18-tpk1

Readout used is Gln3 Gcn4

TF	Interpreted	Simulated	Simulation
Gis1	-	-	0.000
Mig1	-	-	1.411
Dot6	-	-	1.578
Gcn4	On	On	0.955
Rtg13	-	-	0.866
Gln3	On	On	1.000

Description: Zurita-Martinez et al, 2005 studied a *tpk1* strain (MLY41a) grown in YP Glucose + 50nM rapamycin.

Representation:

Preshift Parameters

ATP	1.0
Carbon	1.0
$\text{Glutamine}_{\text{ext}}$	1.0

Postshift Parameters

ATP	1.0
Carbon	1.0
$\text{Glutamine}_{\text{ext}}$	1.0
TORC1_{T}	0.0

Postshift Initial Conditions

TORC1	0

Mutant definition

Parameters

PKA_{T}	0.66

Initial conditions

Model agrees with experiment.

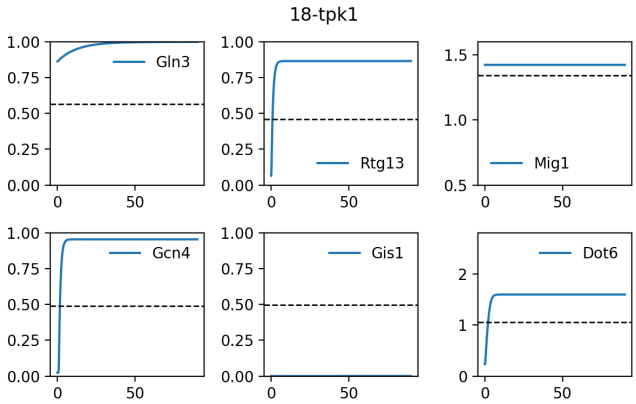

S5.19 19-RAS2v19 gln3 gat1

Readout used is Gln3 Gcn4

TF	Interpreted	Simulated	Simulation
Gis1	-	-	0.000
Mig1	-	-	1.503
Dot6	-	-	1.108
Gcn4	Off	On	0.955
Rtg13	-	-	0.866
Gln3	Off	Off	0.000

Description: Schmelzle et al, 2003 studied a *RAS2v19 gln3 gat1* strain (TB50a) grown in YPD + 200ng/mL rapamycin.

Representation:

Preshift Parameters

ATP	1.0
Carbon	1.0
$\text{Glutamine}_{\text{ext}}$	1.0

Postshift Parameters

ATP	1.0
Carbon	1.0
$\text{Glutamine}_{\text{ext}}$	1.0
TORC1_{T}	0.0

Postshift Initial Conditions

TORC1	0

Mutant definition

Parameters

Gln3_{T}	0.0
w_{raspka}	0.0

Initial conditions

Model does not agree with experiment.

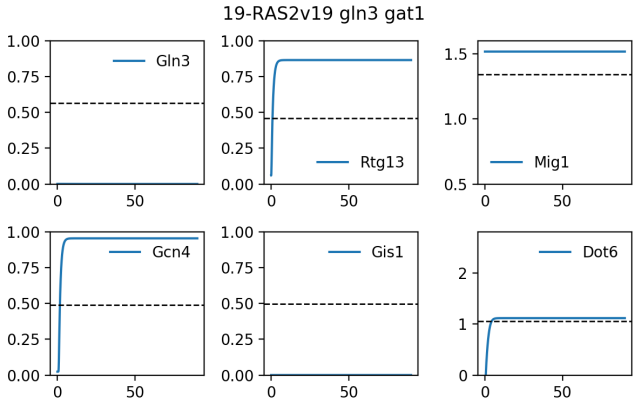

S5.20 20-TPK1 gln3 gat1

Readout used is Gln3 Gcn4

TF	Interpreted	Simulated	Simulation
Gis1	-	-	0.177
Mig1	-	-	1.338
Dot6	-	-	1.874
Gcn4	Off	On	0.955
Rtg13	-	-	0.866
Gln3	Off	Off	0.000

Description: Schmelzle et al, 2003 studied a *TPK1 gln3 gat1* strain (TB50a) grown in YPD + 200ng/mL rapamycin.

Representation:

Preshift Parameters

ATP	1.0
Carbon	1.0
$\text{Glutamine}_{\text{ext}}$	1.0

Postshift Parameters

ATP	1.0
Carbon	1.0
$\text{Glutamine}_{\text{ext}}$	1.0
TORC1_{T}	0.0

Postshift Initial Conditions

TORC1	0

Mutant definition

Parameters

Gln3_{T}	0.0
w_{pkacamp}	0.0

Initial conditions

Model does not agree with experiment.

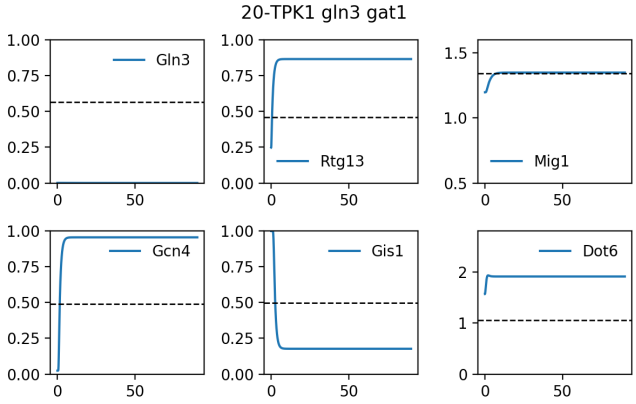

S5.21 21-bcy1

Readout used is Gln3 Gcn4

TF	Interpreted	Simulated	Simulation
Gis1	-	-	0.177
Mig1	-	-	1.338
Dot6	-	-	1.874
Gcn4	On	On	0.955
Rtg13	-	-	0.866
Gln3	On	On	1.000

Description: Schmelzle et al, 2003 studied a *bcy1* strain (TB50a) grown in YPD + 200ng/mL rapamycin.
Representation:

Preshift Parameters

ATP	1.0
Carbon	1.0
$\text{Glutamine}_{\text{ext}}$	1.0

Postshift Parameters

ATP	1.0
Carbon	1.0
$\text{Glutamine}_{\text{ext}}$	1.0
TORC1_{T}	0.0

Postshift Initial Conditions

TORC1	0

Mutant definition

Parameters

w_{pkacamp}	0.0

Initial conditions

Model agrees with experiment.

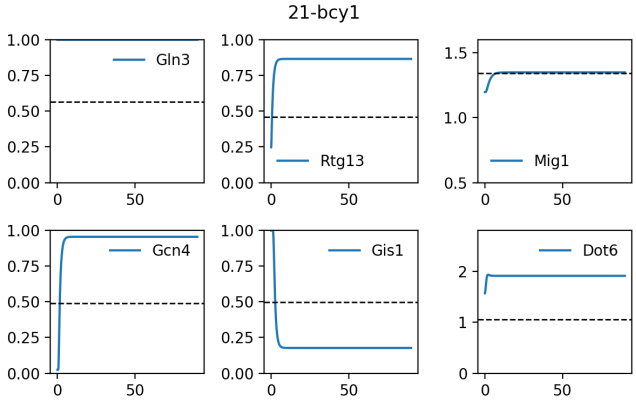

S5.22 22-bcy1 gln3 gat1

Readout used is Gln3 Gcn4

TF	Interpreted	Simulated	Simulation
Gis1	-	-	0.000
Mig1	-	-	1.503
Dot6	-	-	1.108
Gcn4	Off	On	0.955
Rtg13	-	-	0.866
Gln3	Off	Off	0.000

Description: Schmelzle et al, 2003 studied a *bcy1 gln3 gat1* strain (TB50alpha) grown in YPD + 200ng/mL rapamycin.

Representation:

Preshift Parameters

ATP	1.0
Carbon	1.0
$\text{Glutamine}_{\text{ext}}$	1.0

Postshift Parameters

ATP	1.0
Carbon	1.0
$\text{Glutamine}_{\text{ext}}$	1.0
TORC1_{T}	0.0

Postshift Initial Conditions

TORC1	0

Mutant definition

Parameters

Gln3_{T}	0.0
$\text{w}_{\text{pkacamp}}$	1021.0983

Initial conditions

Model does not agree with experiment.

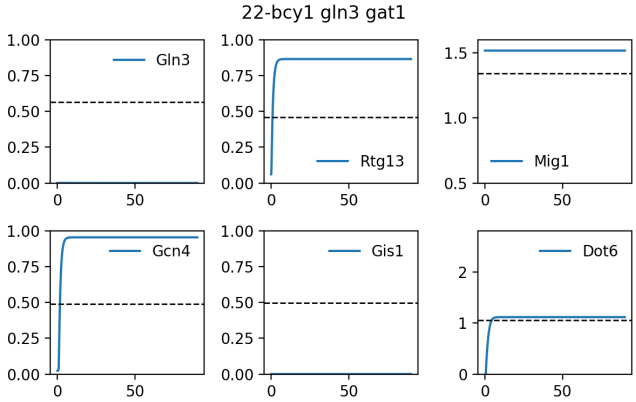

S5.23 23-wt

TF	Interpreted	Simulated	Simulation
Gis1	-	-	0.000
Mig1	-	-	1.503
Dot6	-	-	1.037
Gcn4	On	On	0.806
Rtg13	-	-	0.702
Gln3	-	-	0.999

Description: Cherkasova et al, 2010 studied a *wt* strain (H1642) grown in SC + 10mM 3AT.
Representation:

Preshift Parameters

ATP	1.0
Carbon	1.0
$\text{Glutamine}_{\text{ext}}$	0.0
NH4	2.0

Postshift Parameters

ATP	1.0
Carbon	1.0
$\text{Glutamine}_{\text{ext}}$	0.0
NH4	2.0
k_{accnh4}	0.0001

Postshift Initial Conditions

Mutant definition
Parameters
Initial conditions
Model agrees with experiment.

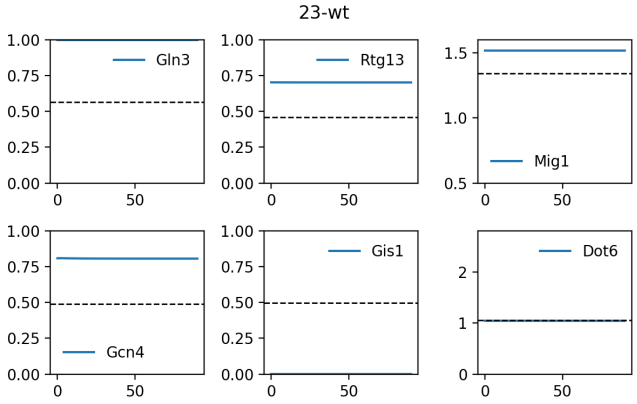

S5.24 24-gcn2

TF	Interpreted	Simulated	Simulation
Gis1	-	-	0.000
Mig1	-	-	1.503
Dot6	-	-	1.037
Gcn4	Off	Off	0.024
Rtg13	-	-	0.702
Gln3	-	-	0.999

Description: Cherkasova et al, 2010 studied a *gcn2* strain (H1895) grown in SC + 10mM 3AT.
Representation:

Preshift Parameters

ATP	1.0
Carbon	1.0
$\text{Glutamine}_{\text{ext}}$	0.0
NH4	2.0

Postshift Parameters

ATP	1.0
Carbon	1.0
$\text{Glutamine}_{\text{ext}}$	0.0
NH4	2.0
k_{accnh4}	0.0001

Postshift Initial Conditions

Mutant definition

Parameters

$Gcn2_T$	0.0

Initial conditions

Model agrees with experiment.

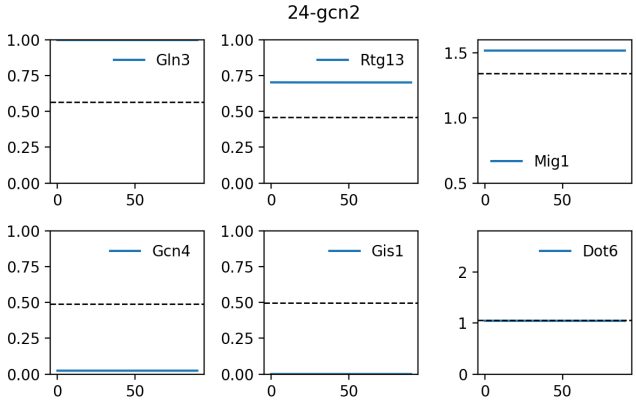

S5.25 25-snf1

TF	Interpreted	Simulated	Simulation
Gis1	-	-	0.000
Mig1	-	-	1.504
Dot6	-	-	1.037
Gcn4	Off	On	0.806
Rtg13	-	-	0.702
Gln3	-	-	0.999

Description: Cherkasova et al, 2010 studied a *snf1* strain (HQY343) grown in SC + 10mM 3AT.
Representation:

Preshift Parameters

ATP	1.0
Carbon	1.0
$Glutamine_{ext}$	0.0
NH4	2.0

Postshift Parameters

ATP	1.0
Carbon	1.0
$Glutamine_{ext}$	0.0
NH4	2.0
k_{accnh4}	0.0001

Postshift Initial Conditions

Mutant definition

Parameters

$Snf1_T$	0.0

Initial conditions

Model does not agree with experiment.

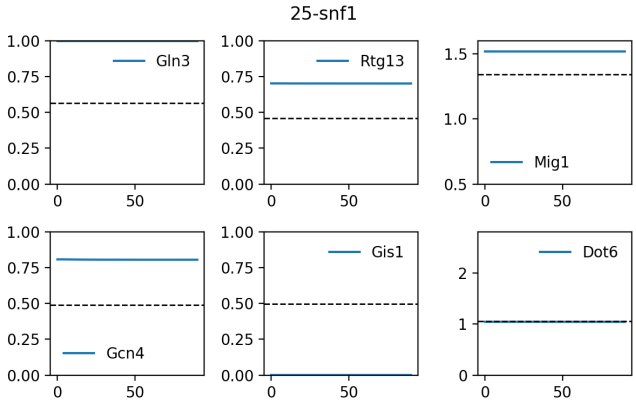

S5.26 26-gcn2 snf1

TF	Interpreted	Simulated	Simulation
Gis1	-	-	0.000
Mig1	-	-	1.504
Dot6	-	-	1.037
Gcn4	Off	Off	0.024
Rtg13	-	-	0.702
Gln3	-	-	0.999

Description: Cherkasova et al, 2010 studied a *gcn2 snf1* strain (HQY344) grown in SC + 10mM 3AT.
Representation:

Preshift Parameters

ATP	1.0
Carbon	1.0
$\text{Glutamine}_{\text{ext}}$	0.0
NH4	2.0

Postshift Parameters

ATP	1.0
Carbon	1.0
$\text{Glutamine}_{\text{ext}}$	0.0
NH4	2.0
k_{accnh4}	0.0001

Postshift Initial Conditions

Mutant definition

Parameters

Gcn2_{T}	0.0
Snf1_{T}	0.0

Initial conditions

Model agrees with experiment.

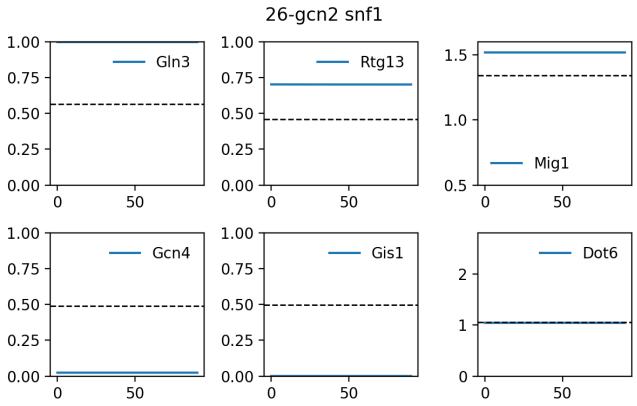

S5.27 27-gln3 gcn4

Readout used is Gln3 Gcn4

TF	Interpreted	Simulated	Simulation
Gis1	-	-	0.000
Mig1	-	-	1.503
Dot6	-	-	1.108
Gcn4	Off	Off	0.000
Rtg13	-	-	0.866
Gln3	Off	Off	0.000

Description: Valenzuela et al, 2001 studied a *gln3 gcn4* strain (CLA-303) grown in YPD 200ng/mL rapamycin.
Representation:

Preshift Parameters

ATP	1.0
Carbon	1.0
$\text{Glutamine}_{\text{ext}}$	1.0

Postshift Parameters

ATP	1.0
Carbon	1.0
$\text{Glutamine}_{\text{ext}}$	1.0
TORC1_{T}	0.0

Postshift Initial Conditions

TORC1	0

Mutant definition

Parameters

$Gcn4_T$	0.0
$Gln3_T$	0.0

Initial conditions

Model agrees with experiment.

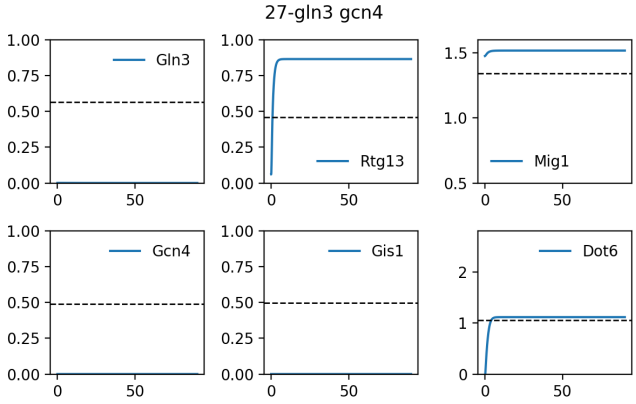

S5.28 28-gcn4

Readout used is Gln3 Gcn4

TF	Interpreted	Simulated	Simulation
Gis1	-	-	0.000
Mig1	-	-	1.503
Dot6	-	-	1.108
Gcn4	On	Off	0.000
Rtg13	-	-	0.866
Gln3	On	On	1.000

Description: Valenzuela et al, 2001 studied a *gcn4* strain (CLA-300) grown in YPD 200ng/mL rapamycin.

Representation:

Preshift Parameters

ATP	1.0
Carbon	1.0
$Glutamine_{ext}$	0.0

Postshift Parameters

ATP	1.0
Carbon	1.0
$Glutamine_{ext}$	1.0
$TORC1_T$	0.0

Postshift Initial Conditions

TORC1	0

Mutant definition

Parameters

$Gcn4_T$	0.0

Initial conditions

Model does not agree with experiment.

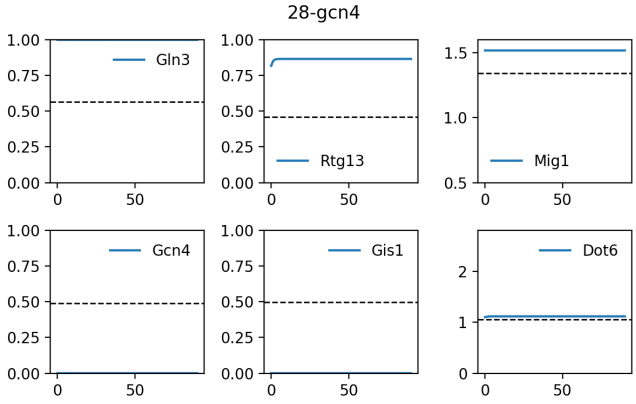

S5.29 29-rph1 gis1

TF	Interpreted	Simulated	Simulation
Gis1	Off	Off	0.000
Mig1	On	On	1.465
Dot6	-	-	-0.048
Gcn4	-	-	0.024
Rtg13	-	-	0.061
Gln3	-	-	0.755

Description: H. Ronne et al, 1999 studied a *rph1 gis1* strain (H874) grown in SD glucose -ura.
Representation:

Preshift Parameters

ATP	1.0
Carbon	1.0
$\text{Glutamine}_{\text{ext}}$	1.0

Postshift Parameters

ATP	1.0
Carbon	1.0
$\text{Glutamine}_{\text{ext}}$	1.0

Postshift Initial Conditions

Mutant definition

Parameters

Gis1_{T}	0.0

Initial conditions

Model agrees with experiment.

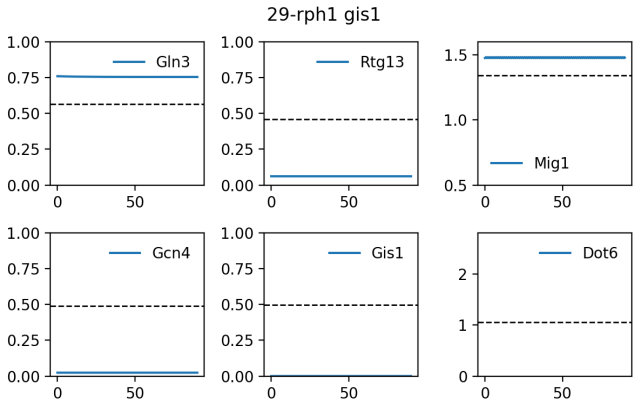

S5.30 30-rph1 gis1

TF	Interpreted	Simulated	Simulation
Gis1	Off	Off	0.000
Mig1	Off	Off	1.168
Dot6	-	-	2.078
Gcn4	-	-	0.608
Rtg13	-	-	0.664
Gln3	-	-	1.000

Description: H. Ronne et al, 1999 studied a *rph1 gis1* strain (H874) grown in YP ethanol.
Representation:

Preshift Parameters

ATP	1.0
Carbon	1.0
$\text{Glutamine}_{\text{ext}}$	1.0

Postshift Parameters

ATP	0.1
Carbon	0.1
$\text{Glutamine}_{\text{ext}}$	1.0

Postshift Initial Conditions

Mutant definition

Parameters

Gis1_{T}	0.0

Initial conditions

Model agrees with experiment.

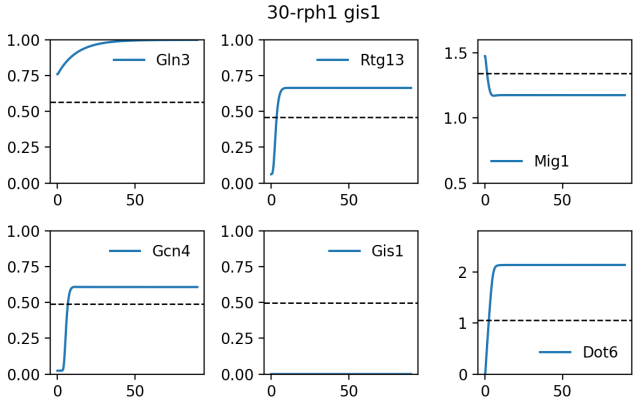

S5.31 34-snf1

Readout used is Gln3 Gcn4

TF	Interpreted	Simulated	Simulation
Gis1	-	-	0.000
Mig1	-	-	1.504
Dot6	-	-	1.108
Gcn4	Off	On	0.955
Rtg13	-	-	0.866
Gln3	Off	On	1.000

Description: Bertram et al, 2002 studied a *snf1* strain (SZy686) grown in YPD + rapamycin.
Representation:

Preshift Parameters

ATP	1.0
Carbon	1.0
$\text{Glutamine}_{\text{ext}}$	1.0

Postshift Parameters

ATP	1.0
Carbon	1.0
$\text{Glutamine}_{\text{ext}}$	1.0
TORC1_{T}	0.0

Postshift Initial Conditions

TORC1	0

Mutant definition

Parameters

Snf1_{T}	0.0

Initial conditions

Model does not agree with experiment.

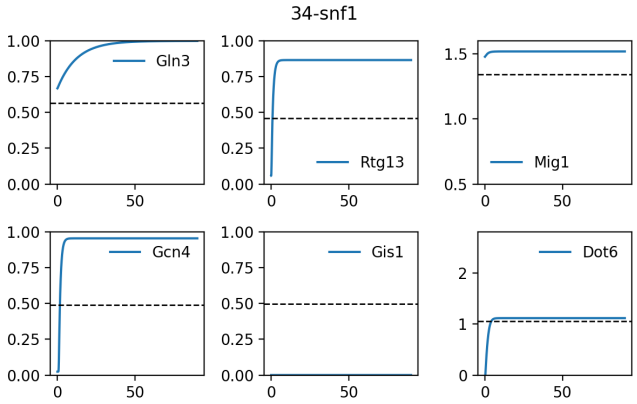

S5.32 35-reg1

Readout used is Gln3 Gcn4

TF	Interpreted	Simulated	Simulation
Gis1	-	-	0.000
Mig1	-	-	1.478
Dot6	-	-	1.108
Gcn4	On	On	0.955
Rtg13	-	-	0.866
Gln3	On	On	1.000

Description: Bertram et al, 2002 studied a *reg1* strain (JC426) grown in YPD + rapamycin.
Representation:

Preshift Parameters

ATP	1.0
Carbon	1.0
$\text{Glutamine}_{\text{ext}}$	1.0

Postshift Parameters

ATP	1.0
Carbon	1.0
$\text{Glutamine}_{\text{ext}}$	1.0
TORC1_{T}	0.0

Postshift Initial Conditions

TORC1	0

Mutant definition

Parameters

w_{snfglc}	0.0

Initial conditions

Model agrees with experiment.

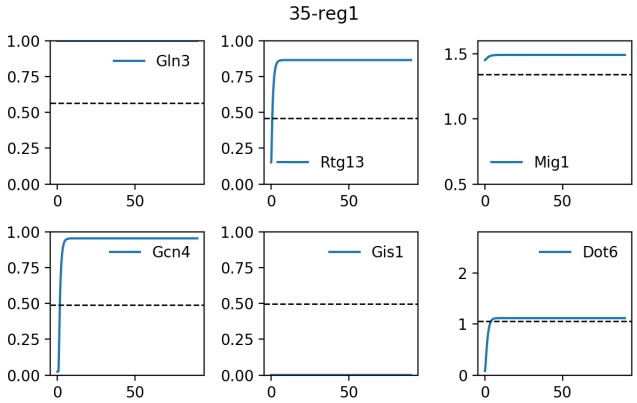

S5.33 36-ure2

Readout used is Gln3 Gcn4

TF	Interpreted	Simulated	Simulation
Gis1	-	-	0.000
Mig1	-	-	1.503
Dot6	-	-	1.108
Gcn4	On	On	0.955
Rtg13	-	-	0.866
Gln3	On	On	1.000

Description: Bertram et al, 2002 studied a *ure2* strain (SZy145) grown in YPD + rapamycin.
Representation:

Preshift Parameters

ATP	1.0
Carbon	1.0
$\text{Glutamine}_{\text{ext}}$	1.0

Postshift Parameters

ATP	1.0
Carbon	1.0
$\text{Glutamine}_{\text{ext}}$	1.0
TORC1_{T}	0.0

Postshift Initial Conditions

TORC1	0

Mutant definition

Parameters

w_{gln3}	0.0

Initial conditions

Model agrees with experiment.

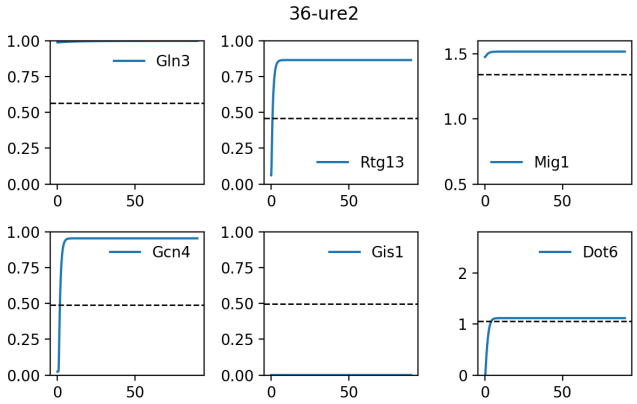

S5.34 37-tap42-11

Readout used is Gln3 Gcn4

TF	Interpreted	Simulated	Simulation
Gis1	-	-	0.000
Mig1	-	-	1.503
Dot6	-	-	1.108
Gcn4	Off	Off	0.398
Rtg13	-	-	0.866
Gln3	Off	On	0.570

Description: Huber et al, 2009 studied a *tap42-11* strain (TB50) grown in YPD + rapamycin.
Representation:

Preshift Parameters

ATP	1.0
Carbon	1.0
$\text{Glutamine}_{\text{ext}}$	1.0

Postshift Parameters

ATP	1.0
Carbon	1.0
$\text{Glutamine}_{\text{ext}}$	1.0
TORC1_{T}	0.0

Postshift Initial Conditions

TORC1	0

Mutant definition

Parameters

w_{gcn}	0.0
w_{glnsit}	0.0

Initial conditions

Model does not agree with experiment.

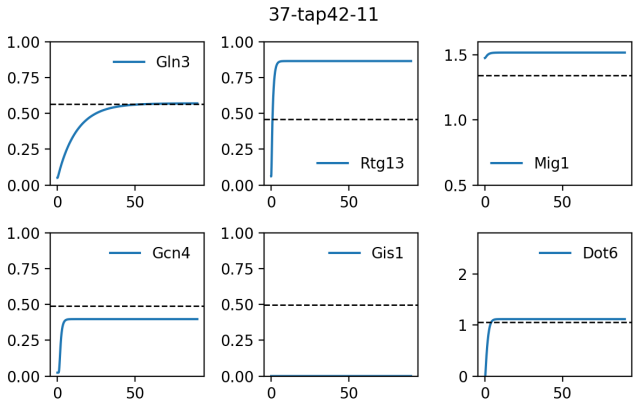

S5.35 38-SCH9^{DE}

Readout used is Gln3 Gcn4

TF	Interpreted	Simulated	Simulation
Gis1	-	-	0.000
Mig1	-	-	1.467
Dot6	-	-	-0.103
Gcn4	Off	Off	0.024
Rtg13	-	-	0.866
Gln3	Off	On	1.000

Description: Huber et al, 2009 studied a *SCH9^{DE}* strain (TB50) grown in YPD + rapamycin.
Representation:

Preshift Parameters

ATP	1.0
Carbon	1.0
$Glutamine_{ext}$	1.0

Postshift Parameters

ATP	1.0
Carbon	1.0
$Glutamine_{ext}$	1.0
$TORC1_T$	0.0

Postshift Initial Conditions

TORC1	0

Mutant definition

Parameters

$Sch9_T$	1.0
w_{sch9}	-10

Initial conditions

Sch9	1.0

Model does not agree with experiment.

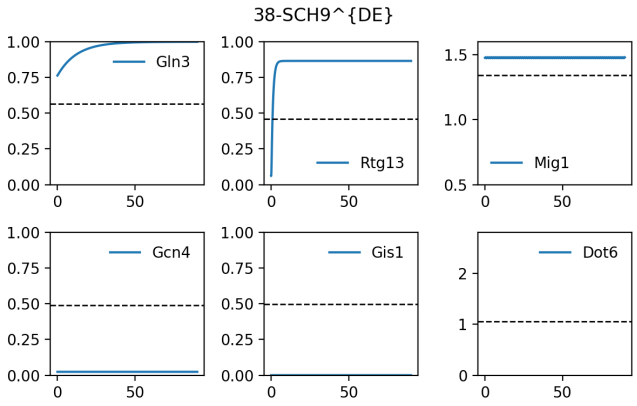

S5.36 39-SCH9^{DE} tap42

TF	Interpreted	Simulated	Simulation
Gis1	-	-	0.000
Mig1	-	-	1.467
Dot6	-	-	-0.103
Gcn4	Off	Off	0.024
Rtg13	-	-	0.866
Gln3	Off	On	0.596

Description: Huber et al, 2009 studied a *SCH9^{DE} tap42* strain (TB50) grown in YPD + rapamycin.
Representation:

Preshift Parameters

ATP	1.0
Carbon	1.0
Glutamine$_{ext}$	1.0

Postshift Parameters

ATP	1.0
Carbon	1.0
Glutamine$_{ext}$	1.0
TORC1$_T$	0.0

Postshift Initial Conditions

TORC1	0

Mutant definition

Parameters

Sch9$_T$	1.0
w$_{sch9}$	-10
w$_{gcn}$	0.0
w$_{glnsit}$	0.0

Initial conditions

Sch9	1.0

Model does not agree with experiment.

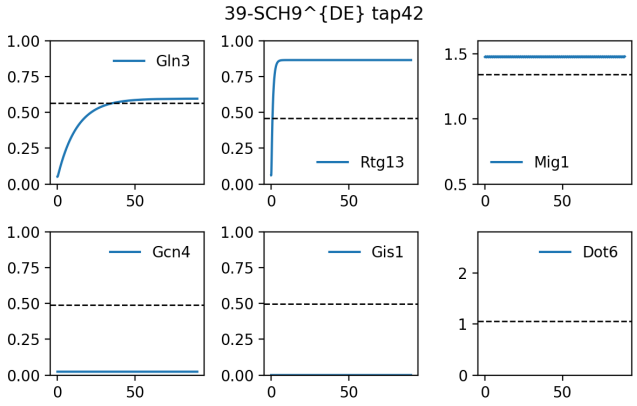

S5.37 40-sch9

TF	Interpreted	Simulated	Simulation
Gis1	On	Off	0.046
Mig1	-	-	1.264
Dot6	-	-	1.825
Gcn4	-	-	0.963
Rtg13	-	-	0.577
Gln3	-	-	1.000

Description: Roosen et al, 2005 studied a *sch9* strain (W303-1) grown in YP + glycerol.
Representation:

Preshift Parameters		*Postshift Parameters*		*Postshift Initial Conditions*
ATP	1.0	ATP	0.01	
Carbon	1.0	Carbon	0.01	
$\text{Glutamine}_{\text{ext}}$	1.0	$\text{Glutamine}_{\text{ext}}$	1.0	

Mutant definition

Parameters		*Initial conditions*	
Sch9_{T}	0.0	Sch9	0.0

Model does not agree with experiment.

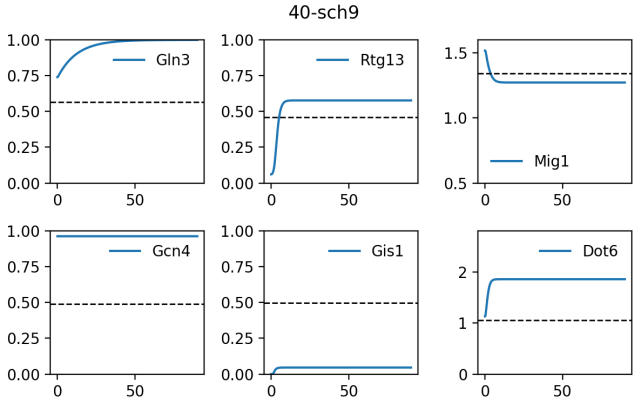

S5.38 41-sch9 gis1

TF	Interpreted	Simulated	Simulation
Gis1	Off	Off	0.000
Mig1	-	-	1.264
Dot6	-	-	1.825
Gcn4	-	-	0.963
Rtg13	-	-	0.577
Gln3	-	-	1.000

Description: Roosen et al, 2005 studied a *sch9 gis1* strain (W303-1) grown in YP + glycerol.
Representation:

Preshift Parameters		*Postshift Parameters*		*Postshift Initial Conditions*
ATP	1.0	ATP	0.01	
Carbon	1.0	Carbon	0.01	
$\text{Glutamine}_{\text{ext}}$	1.0	$\text{Glutamine}_{\text{ext}}$	1.0	

Mutant definition

Parameters		*Initial conditions*	
Gis1_{T}	0.0	Gis1	0.0
Sch9_{T}	0.0	Sch9	0.0

Model agrees with experiment.

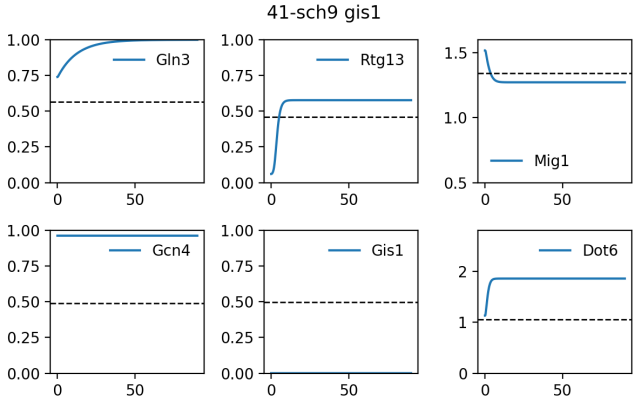
41-sch9 gis1
Gln3
Rtg13
Mig1
Gcn4
Gis1
Dot6

Strain	HCHG						HCHN						HCHP						HCLN					
	Gis1	Mig1	Dot6	Gcn4	Rtg13	Gln3	Gis1	Mig1	Dot6	Gcn4	Rtg13	Gln3	Gis1	Mig1	Dot6	Gcn4	Rtg13	Gln3	Gis1	Mig1	Dot6	Gcn4	Rtg13	Gln3
wt	0	94	4	0	2	1	0	97	70	96	100	100	0	97	72	100	100	100	0	97	72	100	100	100
Δlst4/7	0	94	4	0	2	1	0	97	72	100	100	100	0	97	72	100	100	100	0	97	72	100	100	100
Δsch9	0	97	75	100	2	1	0	97	75	100	100	100	0	97	75	100	100	100	0	97	75	100	100	100
Δgcn2	0	94	4	0	2	1	0	97	70	0	100	100	0	97	72	0	100	100	0	97	72	0	100	100
Δsnf1	0	94	4	0	2	1	0	97	70	96	100	98	0	97	72	100	100	100	0	97	72	100	100	100
Δtpk1/2/3	100	3	75	30	42	100	100	3	75	98	100	100	100	3	75	100	100	100	100	3	75	100	100	100
Δcyr1	100	3	73	29	42	100	71	15	73	97	100	100	31	42	74	100	100	100	29	43	74	100	100	100
Δpde1/2	0	97	2	0	2	1	0	97	70	96	100	100	0	97	72	100	100	100	0	97	72	100	100	100
Δsak1	0	94	4	0	2	1	0	97	70	96	100	100	0	97	72	100	100	100	0	97	72	100	100	100
Δtor1	0	97	73	100	100	100	0	97	73	100	100	100	0	97	73	100	100	100	0	97	73	100	100	100
Δras2	99	3	72	26	41	100	21	50	73	97	100	100	3	70	73	100	100	100	2	71	73	100	100	100
Δgtr1/2	0	96	62	22	82	94	0	97	72	100	100	100	0	97	72	100	100	100	0	97	72	100	100	100
GCN2-S557	0	94	4	100	2	1	0	97	70	100	100	100	0	97	72	100	100	100	0	97	72	100	100	100
GLN3 ΔST	0	94	4	0	2	1	0	97	70	96	100	98	0	97	72	100	100	100	0	97	72	100	100	100
GLN3 ΔTT	0	94	4	0	2	0	0	97	70	96	100	0	0	97	72	100	100	0	0	97	72	100	100	0
Δbcy1	0	97	3	0	2	1	0	97	70	96	100	100	0	97	72	100	100	100	0	97	72	100	100	100
Δira1/2	0	97	2	0	2	1	0	97	70	96	100	100	0	97	72	100	100	100	0	97	72	100	100	100

Strain	LCHG						LCHN						LCHP						LCLN					
	Gis1	Mig1	Dot6	Gcn4	Rtg13	Gln3	Gis1	Mig1	Dot6	Gcn4	Rtg13	Gln3	Gis1	Mig1	Dot6	Gcn4	Rtg13	Gln3	Gis1	Mig1	Dot6	Gcn4	Rtg13	Gln3
wt	100	2	73	68	95	100	67	5	73	99	100	100	21	9	74	100	100	100	21	9	74	100	100	100
Δlst4/7	100	2	73	69	95	100	21	9	74	100	100	100	21	9	74	100	100	100	21	9	74	100	100	100
Δsch9	4	16	75	100	47	96	4	16	75	100	100	100	4	16	75	100	100	100	4	16	75	100	100	100
Δgcn2	100	2	73	0	95	100	67	5	73	0	100	100	21	9	74	0	100	100	21	9	74	0	100	100
Δsnf1	99	9	75	0	2	1	75	34	73	96	100	98	40	55	74	100	100	100	37	56	74	100	100	100
Δtpk1/2/3	100	1	75	73	95	100	100	1	75	99	100	100	100	1	75	100	100	100	100	1	75	100	100	100
Δcyr1	100	2	73	68	95	100	67	5	73	99	100	100	21	9	74	100	100	100	21	9	74	100	100	100
Δpde1/2	100	2	73	68	95	100	67	5	73	99	100	100	21	9	74	100	100	100	21	9	74	100	100	100
Δsak1	99	7	75	0	2	66	74	25	73	97	100	100	32	42	74	100	100	100	30	44	74	100	100	100
Δtor1	19	10	74	100	100	100	19	10	74	100	100	100	19	10	74	100	100	100	19	10	74	100	100	100
Δras2	100	2	73	68	95	100	67	5	73	99	100	100	21	9	74	100	100	100	21	9	74	100	100	100
Δgtr1/2	35	6	74	100	100	100	20	10	74	100	100	100	20	10	74	100	100	100	20	10	74	100	100	100
GCN2-S557	100	2	73	100	95	100	67	5	73	100	100	100	21	9	74	100	100	100	21	9	74	100	100	100
GLN3 ΔST	100	2	73	68	95	92	67	5	73	99	100	98	21	9	74	100	100	100	21	9	74	100	100	100
GLN3 ΔTT	100	2	73	68	95	100	67	5	73	99	100	98	21	9	74	100	100	96	21	9	74	100	100	96
Δbcy1	1	16	60	6	47	96	2	16	73	98	100	100	3	16	74	100	100	100	3	16	74	100	100	100
Δira1/2	100	2	73	68	95	100	67	5	73	99	100	100	21	9	74	100	100	100	21	9	74	100	100	100

Table S5: Summary of predicted global cellular state. Each cell contains the precentage of parameter sets that predicted the given transcription factor to be 'on' in the given strain under a specific nutrient condition. Light colors represent robust predictions where greater than 90% of the parameter sets are in consensus regarding the state of a transcription factor. Bright colors represent fragile predictions. Boxes around cells indicate the presence of experimental data. Solid boxes indicate agreement with experiment while dashed boxes indicate a mismatch. The color of the box indicates the state of the transcription factor as interpreted from experimental data, provided at `https://github.com/amoghpj/nutrient-signaling/blob/master/data/csv/tf-state-experimental-evidence.csv`